JOURNAL OF APPLIED STATISTICS
2021, VOL. 48, NO. 12, 2178–2204
https://doi.org/10.1080/02664763.2020.1787356

Taylor & Francis
Taylor & Francis Group

Monitoring coefficient of variation using one-sided run rules control charts in the presence of measurement errors

Phuong Hanh Tran [a], Cédric Heuchenne[a], Huu Du Nguyen[b] and Hélène Marie[c,d]

[a]HEC Liège – Management School of the University of Liège, Liège, Belgium; [b]Institute of Artificial Intelligence and Data Science, Dong A University, Danang, Vietnam; [c]Informetrics Research Group, Ton Duc Thang University, Ho Chi Minh City, Vietnam; [d]Faculty of Business Administration, Ton Duc Thang University, Ho Chi Minh City, Vietnam

ABSTRACT

We investigate, in this paper, the effect of the measurement error (ME) on the performance of Run Rules control charts monitoring the coefficient of variation (CV) squared. The previous Run Rules CV chart in the literature is improved slightly by monitoring the CV squared using two one-sided Run Rules charts instead of monitoring the CV itself using a two-sided chart. The numerical results show that this improvement gives better performance in detecting process shifts. Moreover, we will show through simulation that the *precision* and *accuracy* errors do have a negative effect on the performance of the proposed Run Rules charts. We also find out that taking multiple measurements per item is not an effective way to reduce these negative effects. The proposed Run Rules control charts can be applied in the anomaly detection area.

ARTICLE HISTORY
Received 8 December 2019
Accepted 21 June 2020

KEYWORDS
Run rules chart; Markov chain; coefficient of variation; measurement errors; anomaly detection

1. Introduction

Among important statistical characteristics of a variable, the coefficient of variation (CV) is widely used to evaluate the stability or concentration of the random variable around the mean. It is defined as the ratio between the standard deviation to the mean, $\gamma = \sigma/\mu$. In many industrial processes, keeping the value of this coefficient of a characteristic of interest within the permissible range means assuring the quality of products. A number of examples have been illustrated in the literature for the applications of the CV in industry. Castagliola *et al.* [5] presented an example where the quality of interest is the pressure test drop time from a sintering process manufacturing mechanical parts. In this example, the presence of a constant proportionality between the standard deviation of the pressure drop time and its mean was confirmed. The CV was then monitored to detect changes in the process variability. Ye *et al.* [22] showed that it is useful to monitor the CV in detecting the presence of chatter, a severe form of self-excited vibration in the machining process which leads to many machining problems. More examples about the need of using the CV as a measure of interest has been discussed in [10]. Because of its wide range of applications, monitoring the CV has been a major objective in many studies in statistical process control,

CONTACT Phuong Hanh Tran phtran@uliege.be

see, for example, Castagliola *et al.* [3], Zhang *et al.* [26], Castagliola *et al.* [4], Yeong *et al.* [23], Tran and Tran [20], Khaw *et al.* [8], Noor-ul Amin *et al.* [13] and Noor-ul Amin and Riaz [12].

Along with the development of the advanced control charts monitoring the CV with improved performance, recent researches are paying attention to the effect of the measurement error on the CV control chart. This makes these researches become more in touch reality since the measurement error is often present in practice. A Shewhart control chart monitoring the CV under the presence of measurement error (ME) was suggested by Yeong *et al.* [24]. Tran *et al.* [19] improved the linear covariate error model for the CV in [24] and then proposed the EWMA CV control chart with ME. Also, researchers studied the effect of ME on the variable sampling interval control chart [11], the cumulative sum control chart monitoring the CV [18], and the hotelling T2 control chart [25]. Very recently, Shongwe *et al.* [14] proposed a combined mixed-s-skip sampling strategy to reduce the effect of autocorrelation on the X-bar in the presence of measurement errors.

One of the reasons leads to the introduction of many advanced control charts monitoring the CV is to overcome a drawback of the Shewhart CV chart which is only sensitive to the large shifts. However, the Shewhart chart is still popularly used thanks to its simplicity in implementation. From this point of view, the Run Rules charts are advantageous: they are easy to implement (compared to, for example, the EWMA control chart or the CUSUM control chart, even these charts may bring better performance) and they can improve remarkably the performance of the Shewhart chart in detecting small or moderate process shifts. The aim of this paper is to investigate the performance of Run Rules CV control chart under the presence of ME. In fact, the Run Rules chart monitoring the CV has been studied in [2]. However, the ME has not been considered. Moreover, in this study, the authors only focused on the two-sided charts (the one-sided chart has been mentioned, but quite sketchily without explanation for the design) with the CV monitored directly. We improve this design by monitoring the CV squared and presenting the design of the two one-sided Run Rules charts in detail.

The paper proposes new advanced control charts that can be applied for anomaly detection. This issue has scored a blooming in science community recently. It has been seen a connection between control chart and anomaly detection to improve the quality of credit card management [21] or process in various areas [27], and to track the behaviour of emergency department [7]. Anomaly detection is defined as a notion of finding instances in data that are difference in compare with expected behavior. Approaches based on anomaly detection perspective have contributed to increased efficiency in the decision making process.

This paper consists of eight sections and is organized as follows. Followed by the introduction in Section 1, Section 2 presents a brief review of the distribution of the sample coefficient of variation. The design and the implementation of two one-sided Run Rules control charts monitoring the CV squared (denoted as $\mathrm{RR}_{r,s} - \gamma^2$ charts) are presented in Section 3. Section 4 is for the performance of these charts. A linear covariate error model for the CV is reintroduced in Section 5. The design of control charts in the presence of measurement errors and the effect of the measurement error on the $\mathrm{RR}_{r,s} - \gamma^2$ charts are displayed in Section 6. Section 7 is devoted to an illustrative example. Some concluding remarks are given in Section 8 to conclude.

2. A brief review of distribution of the sample coefficient of variation

In this section, the distribution of the CV is briefly presented. The CV of a random variable X, say γ, is defined as the ratio of the standard deviation $\sigma = \sigma(X)$ to the mean $\mu = E(X)$; i.e.

$$\gamma = \frac{\sigma}{\mu}.$$

Suppose that a sample of size n of normal i.i.d. random variables $\{X_1, \ldots, X_n\}$ is collected. Let $\bar{X}$ and S be the sample mean and the sample standard deviation of these variables, i.e.

$$\bar{X} = \frac{1}{n}\sum_{i=1}^{n} X_i$$

and

$$S = \sqrt{\frac{1}{n-1}\sum_{i=1}^{n}(X_i - \bar{X})^2}.$$

Then, the sample coefficient of variation $\hat{\gamma}$ of these variables is defined as

$$\hat{\gamma} = \frac{S}{\bar{X}}.$$

The probability distribution of the sample CV $\hat{\gamma}$ has been studied in the literature by many authors. However, the exact distribution of $\hat{\gamma}$ has a complicated form. The approximate distribution is then widely used as an alternative. The approximation of $F_{\hat{\gamma}}(x|n,\gamma)$, the *c.d.f* (cumulative distribution function) of $\hat{\gamma}$, which is suggested by Castagliola *et al.* [5]:

$$F_{\hat{\gamma}}(x \mid n,\gamma) \simeq 1 - F_t\left(\frac{\sqrt{n}}{x}\middle| n-1, \frac{\sqrt{n}}{\gamma}\right), \tag{1}$$

where $F_t(.|n-1, \sqrt{n}/\gamma)$ is the c.d.f. of the noncentral t distribution with $n-1$ degrees of freedom and noncentrality parameter. This approximation is only sufficiently precise when $\gamma < 0.5$. This condition is in general satisfied in our case as it is very frequent that the CV takes small values to ensure the stability of a process. More details on this problem have been discussed in [19].

For the case of the sample CV squared ($\hat{\gamma}^2$), Castagliola *et al.* [5] showed that $n/\hat{\gamma}^2$ follows a noncentral F distribution with $(1, n-1)$ degrees of freedom and noncentrality parameter n/γ^2. Then, they deduced the *c.d.f* $F_{\hat{\gamma}^2}(x \mid n,\gamma)$ of $\hat{\gamma}^2$ as

$$F_{\hat{\gamma}^2}(x|n,\gamma) = 1 - F_F\left(\frac{n}{x}\middle| 1, n-1, \frac{n}{\gamma^2}\right), \tag{2}$$

where $F_F\left(.|1, n-1, n/\gamma^2\right)$ is the *c.d.f* of the noncentral F distribution. The corresponding density function of $\hat{\gamma}^2$ is then

$$f_{\hat{\gamma}^2}(x \mid n,\gamma) = \frac{n}{x^2} f_F\left(\frac{n}{x}\middle| 1, n-1, \frac{n}{\gamma^2}\right), \tag{3}$$

where $f_F\left(.|1, n-1, n/\gamma^2\right)$ is the density function of the noncentral F distribution.

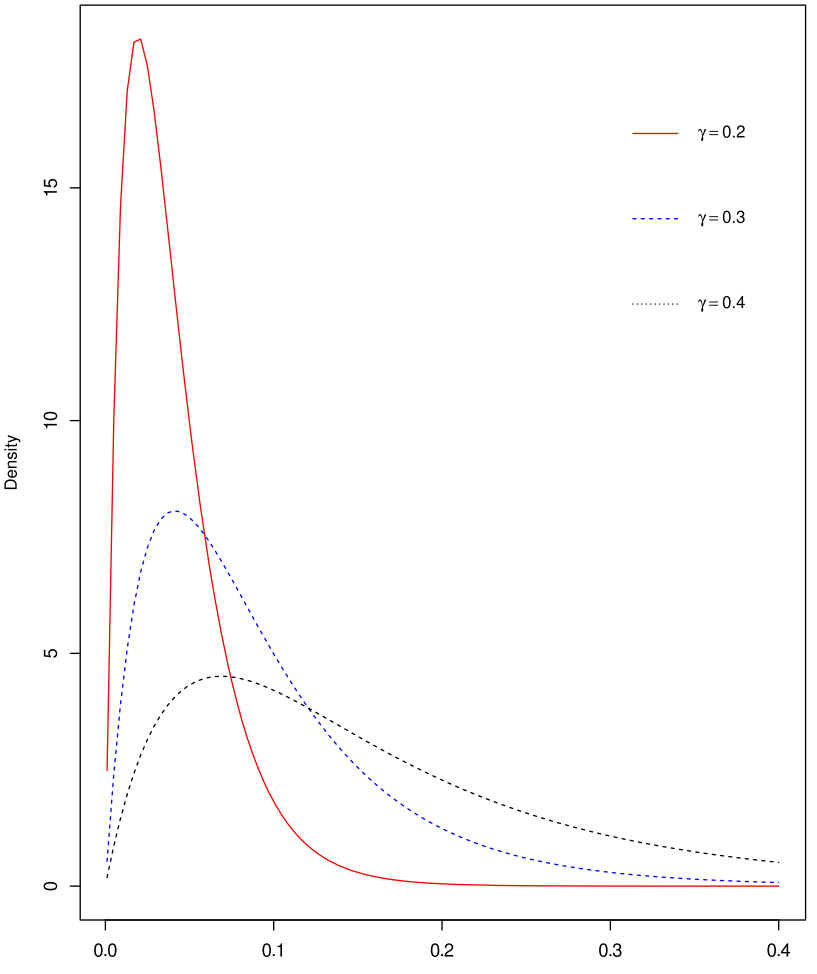

Figure 1. The approximate density function of the $\hat{\gamma}^2$ for $n = 5$.

Figure 1 presents the density distribution of γ^2 for $n = 5$ and some different values of γ.

3. Design and implementation of the $RR_{r,s} - \gamma^2$ control chart

In the literature, the Run Rules control charts monitoring the CV have been investigated in [2] with two-sided charts. However, since the distribution of γ^2 is asymmetric (as can be seen from Equation (2) and also from Figure 1), these two-sided charts lead to the problem of *ARL*-biased (Average Run Length) performance, i.e. the out-of-control ARL_1 values are larger than the in-control values ARL_0. This problem was also pointed out in [2]. It is important to note that *ARL* is defined as the average number of samples before the first out-of-control point is plotted in the control chart with a given specific shift τ [17]. *ARL* is concerned at the zero-state of the investigated statistical measure of performance. ARL_0 and ARL_1 are denoted for the value of ARL when a process is in-control and out-of-control, respectively. It is expected that the control chart has the smallest ARL_1 value at a

specific shift τ and when ARL_0 is the same for all the charts. Therefore, we overcome the *ARL*-biased property by designing simultaneously two one-sided charts to detect both the increase and decrease of the CV squared. In particular, we suggest defining two one-sided Run Rules control charts monitoring the CV squared, involving:

- a lower-sided r-out-of-s Run Rules control chart (denoted as $\text{RR}^-_{r,s} - \gamma^2$) to detect a decrease in γ with a lower control limit $LCL^- = \mu_0(\hat{\gamma}^2) - k_d.\sigma_0(\hat{\gamma}^2)$ and an upper control limit $UCL^- = +\infty$,
- an upper-sided r-out-of-s Run Rules control chart (denoted as $\text{RR}^+_{r,s} - \gamma^2$) to detect an increase in γ with a lower control limit $UCL^+ = \mu_0(\hat{\gamma}^2) + k_u.\sigma_0(\hat{\gamma}^2)$ and a lower control limit $LCL^+ = 0$,

where $k_d > 0$ and $k_u > 0$ are the chart parameters of the $\text{RR}^-_{r,s} - \gamma^2$ and $\text{RR}^+_{r,s} - \gamma^2$ charts, respectively.

The closed forms of $\mu_0(\hat{\gamma}^2)$ and $\sigma_0(\hat{\gamma}^2)$ have not been presented in the literature. We apply in this study the accurate approximations provided by Breunig [1] for both $\mu_0(\hat{\gamma}^2)$ and $\sigma_0(\hat{\gamma}^2)$ as follows:

$$\mu_0(\hat{\gamma}^2) = \gamma_0^2\left(1 - \frac{3\gamma_0^2}{n}\right), \tag{4}$$

$$\sigma_0(\hat{\gamma}^2) = \sqrt{\gamma_0^4\left(\frac{2}{n-1} + \gamma_0^2\left(\frac{4}{n} + \frac{20}{n(n-1)} + \frac{75\gamma_0^2}{n^2}\right)\right) - (\mu_0(\hat{\gamma}^2) - \gamma_0^2)^2}. \tag{5}$$

Given the value of the control limit for each chart, an out-of-control signal is given at time i if r-out-of-s consecutive $\hat{\gamma}_i$ values are plotted outside the control interval, i.e. $\hat{\gamma}_i^2 < LCL^-$ in the lower-sided chart and $\hat{\gamma}_i^2 > UCL^+$ in the upper-sided chart. The control charts designed above are called *pure* Run Rules type chart. In this study, we only consider the 2-out-of-3, 3-out-of-4 and 4-out-of-5 Run Rules charts. The performance of the proposed charts is measured by the *ARL* which is calculated by using Markov chain as follows.

Firstly, we define the matrix $\mathbf{P}$ of the embedded Markov chain. For the two one-sided $\text{RR}_{2,3} - \gamma^2$ control charts, $\mathbf{P}$ is defined by

$$\mathbf{P} = \begin{pmatrix} \mathbf{Q} & \mathbf{r} \\ \mathbf{0}^T & 1 \end{pmatrix} = \left(\begin{array}{ccc|c} 0 & 0 & p & 1-p \\ p & 0 & 0 & 1-p \\ 0 & 1-p & p & 0 \\ \hline 0 & 0 & 0 & 1 \end{array}\right), \tag{6}$$

where $\mathbf{Q}$ is a $(3, 3)$ matrix of transient probabilities, $\mathbf{r}$ is a $(3, 1)$ vector satisfied $\mathbf{r} = \mathbf{1} - \mathbf{Q1}$ with $\mathbf{1} = (1, 1, 1)^{\mathrm{T}}$ and $\mathbf{0} = (0, 0, 0)^{\mathrm{T}}$, p is the probability that a sample drops into the control interval. The corresponding $(3, 1)$ vector $\mathbf{q}$ of initial probabilities associated with the transient states is $\mathbf{q} = (0, 0, 1)^{\mathrm{T}}$, i.e. the third state is the initial state.

For the case of $RR_{3,4} - \gamma^2$ control charts, the transient probability matrix $\mathbf{Q}_{(7\times7)}$ is given by

$$\mathbf{Q} = \begin{pmatrix} 0 & 0 & p & 0 & 0 & 0 & 0 \\ 0 & 0 & 0 & 0 & p & 0 & 0 \\ 0 & 0 & 0 & 0 & 0 & 1-p & p \\ p & 0 & 0 & 0 & 0 & 0 & 0 \\ 0 & 1-p & p & 0 & 0 & 0 & 0 \\ 0 & 0 & 0 & 1-p & p & 0 & 0 \\ 0 & 0 & 0 & 0 & 0 & 1-p & p \end{pmatrix}. \tag{7}$$

In this case, the seventh state in the vector $\mathbf{q} = (0, 0, 0, 0, 0, 0, 1)^{\mathrm{T}}$ is the initial state.

Extended to 'longer' (4, 5) Run Rules, the (15, 15) matrix $\mathbf{Q}$ of transient probabilities for the two one-sided $RR_{4,5} - \gamma^2$ control charts is

$$\mathbf{Q} = \begin{pmatrix} 1-p & p & 0 & 0 & 0 & 0 & 0 & p \\ 0 & 0 & p & 1-p & 0 & 0 & 0 & 0 \\ 0 & 0 & 0 & 0 & p & 1-p & 0 & 0 \\ 0 & 0 & 0 & 0 & 0 & 0 & 1-p & p \\ 0 & 0 & 0 & 0 & 0 & 0 & 0 & 0 \\ 0 & 0 & 0 & 0 & 0 & 0 & 0 & 0 \\ 0 & 0 & 0 & 0 & 0 & 0 & 0 & 0 \\ 0 & 0 & 0 & 0 & 0 & 0 & 0 & 1-p \\ 0 & 0 & 0 & 0 & 0 & 0 & 1-p & p \\ 0 & 0 & 0 & 0 & p & 1-p & 0 & 0 \\ 0 & 0 & p & 1-p & 0 & 0 & 0 & 0 \\ 1-p & p & 0 & 0 & 0 & 0 & 0 & 0 \\ 0 & 0 & 0 & 0 & 0 & 0 & 0 & 0 \\ 0 & 0 & 0 & 0 & 0 & 0 & 0 & 0 \\ 0 & 0 & 0 & 0 & 0 & 0 & 0 & 0 \end{pmatrix}$$

$$\begin{pmatrix} 0 & 0 & 0 & 0 & 0 & 0 & 0 \\ 0 & 0 & 0 & 0 & 0 & 0 & 0 \\ 0 & 0 & 0 & 0 & 0 & 0 & 0 \\ 0 & 0 & 0 & 0 & 0 & 0 & 0 \\ 0 & 0 & 0 & 0 & 0 & 0 & 1-p \\ 0 & 0 & 0 & 0 & p & 1-p & 0 \\ 0 & 0 & 0 & p & 1-p & 0 & 0 \\ p & 0 & 0 & 0 & 0 & 0 & 0 \\ 0 & 0 & 0 & 0 & 0 & 0 & 0 \\ 0 & 0 & 0 & 0 & 0 & 0 & 0 \\ 0 & 0 & 0 & 0 & 0 & 0 & 0 \\ 0 & 0 & 0 & 0 & 0 & 0 & 0 \\ 0 & 1-p & p & 0 & 0 & 0 & 0 \\ 0 & 0 & 0 & p & 1-p & 0 & 0 \\ 0 & 0 & 0 & 0 & 0 & p & 1-p \end{pmatrix}, \tag{8}$$

that corresponds to the $(15, 1)$ initial probabilites vector $\mathbf{q} = (0, \ldots, 0, 1)^{\mathrm{T}}$ (i.e. the initial state is the 15th one). These transient probability matrices has been presented in, for example, [15–17].

Let us now suppose that the occurrence of an unexpected condition shifts the in-control CV value γ_0 to the out-of-control value $\gamma_1 = \tau \times \gamma_0$, where $\tau > 0$ is the shift size. Values of $\tau \in (0, 1)$ correspond to a decrease of the γ_0, while values of $\tau > 1$ correspond to an increase of γ_0. Then, the probability p is defined by

- for the $\mathrm{RR}^{-}_{r,s} - \gamma^2$ chart:

$$p = P(\hat{\gamma}_i^2 \geq LCL^{-}) = 1 - F_{\hat{\gamma}^2}(LCL^{-}|n, \gamma_1), \tag{9}$$

- for the $\mathrm{RR}^{+}_{r,s} - \gamma^2$ chart:

$$p = P(\hat{\gamma}_i^2 \leq UCL^{+}) = F_{\hat{\gamma}^2}(UCL^{+}|n, \gamma_1), \tag{10}$$

where $F_{\hat{\gamma}^2}$ is defined in (2).

Once the matrix $\mathbf{Q}$ and the vector $\mathbf{q}$ have been determined, the *ARL* and the *SDRL* (standard deviation of run length) are calculated by

$$ARL = \mathbf{q}^T(\mathbf{I} - \mathbf{Q})^{-1}\mathbf{1}, \tag{11}$$

$$SDRL = \sqrt{2\mathbf{q}^T(\mathbf{I} - \mathbf{Q})^{-2}\mathbf{Q}\mathbf{1} - ARL^2 + ARL}. \tag{12}$$

It is customary that a control chart is considered to be better than its competitors if it gives a smaller value of the ARL_1 while the ARL_0 is the same. Therefore, the parameters of the $\mathrm{RR}_{r,s} - \gamma^2$ control charts should be the solution of the following equations:

- for the $\mathrm{RR}^{-}_{r,s} - \gamma^2$ chart:

$$ARL(k_d, n, p, \gamma_0, \tau = 1) = ARL_0, \tag{13}$$

- for the $\mathrm{RR}^{+}_{r,s} - \gamma^2$ chart:

$$ARL(k_u, n, p, \gamma_0, \tau = 1) = ARL_0, \tag{14}$$

where ARL_0 is predefined.

4. Performance of $\mathrm{RR}_{r,s} - \gamma^2$ control charts

Assigning the in-control value ARL_0 at $ARL_0 = 370.4$, the parameters k_d and k_u of the lower-sided and upper-sided $\mathrm{RR}_{r,s} - \gamma^2$ charts for some combinations of $n \in \{5, 15\}$, $\gamma_0 \in \{0.05, 0.1, 0.2\}$ are presented in Table 1. Table 2 shows the corresponding ARL_1 values of the proposed charts for various situations of the shift size τ. The obtained results show that the two one-sided $\mathrm{RR}_{r,s} - \gamma^2$ charts not only overcome the *ARL*-biased problem (as the ARL_1 values are always smaller than the ARL_0) but also outperform the two-sided RR-γ charts investigated in [2]. For example, with $\gamma_0 = 0.05, \tau = 1.10$ and $n = 5$ in the $\mathrm{RR}_{2,3} - \gamma^2$ chart, we have $ARL_1 = 95.9$ (Table 2 in this study), which is smaller than $ARL_1 = 101.6$ (Table 2 in [2]).

Table 1. Values of the parameters k_d (left side) and k_u (right side) of the downward chart and the upward $RR_{r,s} - \gamma^2$ charts for $\gamma_0 = \{0.05, 0.1, 0.2\}$ and $n = \{5, 15\}$ when $ARL_0 = 370.4$.

	$\gamma_0 = 0.05$		$\gamma_0 = 0.1$		$\gamma_0 = 0.2$	
Charts	$n = 5$	$n = 15$	$n = 5$	$n = 15$	$n = 5$	$n = 15$
$RR_{2,3} - \gamma^2$	(1.194, 2.167)	(1.487, 2.010)	(1.170, 2.183)	(1.464, 2.023)	(1.088, 2.245)	(1.407, 2.069)
$RR_{3,4} - \gamma^2$	(1.023, 1.293)	(1.159, 1.298)	(1.003, 1.301)	(1.143, 1.306)	(0.930, 1.331)	(1.098, 1.333)
$RR_{4,5} - \gamma^2$	(0.866, 0.801)	(0.915, 0.872)	(0.849, 0.808)	(0.902, 0.878)	(0.785, 0.832)	(0.865, 0.899)

Table 2. Values of $(ARL_1, SDRL_1)$ of $RR_{r,s} - \gamma^2$ charts corresponding to the chart parameters in Table 1 for various situations of τ.

		$\gamma_0 = 0.05$		$\gamma_0 = 0.1$		$\gamma_0 = 0.2$	
Charts	τ	$n = 5$	$n = 15$	$n = 5$	$n = 15$	$n = 5$	$n = 15$
$RR^{-}_{2,3} - \gamma^2$	0.5	(8.1, 6.6)	(2.1, 0.3)	(8.1, 6.5)	(2.1, 0.3)	(8.2, 6.7)	(2.1, 0.3)
$RR^{-}_{3,4} - \gamma^2$		(5.6, 3.3)	(3.0, 0.1)	(5.6, 3.3)	(3.0, 0.1)	(5.7, 3.4)	(3.0, 0.1)
$RR^{-}_{4,5} - \gamma^2$		(5.4, 2.1)	(4.0, 0.1)	(5.4, 2.1)	(4.0, 0.1)	(5.4, 2.2)	(4.0, 0.1)
$RR^{-}_{2,3} - \gamma^2$	0.65	(26.9, 25.2)	(3.8, 2.3)	(26.6, 25.0)	(3.8, 2.2)	(27.1, 25.5)	(3.9, 2.4)
$RR^{-}_{3,4} - \gamma^2$		((16.2, 13.7)	(3.8, 1.4)	(16.2, 13.8)	(3.8, 1.4)	(16.6, 14.1)	(3.9, 1.5)
$RR^{-}_{4,5} - \gamma^2$		(12.6, 9.5)	(4.5, 1.0)	(12.7, 9.6)	(4.5, 1.0)	(13.0, 9.9)	(4.5, 1.0)
$RR^{-}_{2,3} - \gamma^2$	0.8	(87.9, 86.1)	(17.9, 16.2)	(87.2, 85.4)	(17.5, 15.9)	(88.4, 86.6)	(18.2, 16.5)
$RR^{-}_{3,4} - \gamma^2$		(59.8, 57.1)	(12.6, 10.2)	(59.9, 57.2)	(12.7, 10.3)	(61.1, 58.4)	(13.2, 10.8)
$RR^{-}_{4,5} - \gamma^2$		(46.8, 43.4)	(11.1, 8.0)	(47.0, 43.6)	(11.2, 8.0)	(48.1, 44.7)	(11.6, 8.4)
$RR^{-}_{2,3} - \gamma^2$	0.9	(184.4, 182.5)	(75.4, 73.7)	(183.7, 181.9)	(73.9, 72.2)	(185.2, 183.4)	(75.7, 73.9)
$RR^{-}_{3,4} - \gamma^2$		(149.3, 146.5)	(55.4, 52.7)	(149.5, 146.7)	(55.3, 52.6)	(151.3, 148.5)	(57.1, 54.5)
$RR^{-}_{4,5} - \gamma^2$		(128.7, 125.1)	(46.5, 43.1)	(129.1, 125.4)	(46.7, 43.3)	(130.9, 127.3)	(48.3, 44.9)
$RR^{+}_{2,3} - \gamma^2$	1.10	(95.9, 94.1)	(45.8, 44.1)	(96.5, 94.7)	(46.4, 44.6)	(98.7, 96.9)	(48.5, 46.8)
$RR^{+}_{3,4} - \gamma^2$		(94.2, 91.5)	(42.3, 39.7)	(94.8, 92.0)	(42.8, 40.1)	(97.0, 94.2)	(44.7, 42.1)
$RR^{+}_{4,5} - \gamma^2$		(94.9, 91.4)	(41.3, 37.9)	(95.4, 91.9)	(41.7, 38.3)	(97.6, 94.0)	(43.6, 40.2)
$RR^{+}_{2,3} - \gamma^2$	1.25	(25.8, 24.2)	(8.7, 7.1)	(26.1, 24.4)	(8.8, 7.2)	(27.2, 25.6)	(9.4, 7.8)
$RR^{+}_{3,4} - \gamma^2$		(26.3, 23.8)	(8.9, 6.5)	(26.5, 24.0)	(9.0, 6.6)	(27.6, 25.1)	(9.5, 7.1)
$RR^{+}_{4,5} - \gamma^2$		(27.5, 24.2)	(9.5, 6.4)	(27.8, 24.5)	(9.6, 6.5)	(28.9, 25.5)	(10.1, 7.0)
$RR^{+}_{2,3} - \gamma^2$	1.5	(8.1, 6.6)	(3.1, 1.5)	(8.2, 6.7)	(3.1, 1.6)	(8.6, 7.1)	(3.3, 1.7)
$RR^{+}_{3,4} - \gamma^2$		(9.1, 6.7)	(3.9, 1.4)	(9.2, 6.8)	(3.9, 1.5)	(9.6, 7.2)	(4.0, 1.6)
$RR^{+}_{4,5} - \gamma^2$		(10.2, 7.1)	(4.8, 1.4)	(10.3, 7.2)	(4.8, 1.4)	(10.7, 7.6)	(4.9, 1.6)
$RR^{+}_{2,3} - \gamma^2$	2.0	(3.4, 1.9)	(2.1, 0.3)	(3.4, 1.9)	(2.1, 0.3)	(3.6, 2.1)	(2.1, 0.4)
$RR^{+}_{3,4} - \gamma^2$		(4.3, 2.0)	(3.1, 0.3)	(4.4, 2.0)	(3.1, 0.3)	(4.6, 2.2)	(3.1, 0.3)
$RR^{+}_{4,5} - \gamma^2$		(5.3, 2.1)	(4.0, 0.2)	(5.4, 2.1)	(4.0, 0.2)	(5.6, 2.3)	(4.1, 0.3)

5. Linear covariate error model for the coefficient of variation

The previous design for the $RR_{r,s} - \gamma^2$ control charts is based on a latent assumption that the values in the collected sample are measured exactly without the measurement error. This assumption, however, is usually not reached in practice and it is difficult to avoid the measurement error. In this section, we suppose a linear covariate error model to the measurement error, which is suggested by Linna and Woodall [9].

Suppose that the quality characteristic X of n consecutive items at step ith is $(X_{i,1}, X_{i,2}, \ldots, X_{i,n})$, where $X_{i,j} \sim N(\mu_0 + a\sigma_0, b^2\sigma_0^2)$, where μ_0 and σ_0 are the in-control

mean and standard deviation of X, a and b represent the standardized mean and the standardized deviation shifts, respectively. The process has shifted if the process mean μ_0 and/or the process standard deviation σ_0 have changed ($a \neq 0$ and/or $b \neq 1$). Due to the measurement error, we only observe the values $(X^*_{i,j,1}, \ldots, X^*_{i,j,m})$ of a set of m measurement operations instead the true values $X_{i,j}$. According to the linear covariate error model, we assume $X^*_{i,j,k} = A + BX_{i,j} + \varepsilon_{i,j,k}$, where A and B are two known constants and $\varepsilon_{i,j,k}$ is a normal random error term with parameters $(0, \Sigma_M)$ and independent of $X_{i,j}$. Note that A is the constant bias component and B represents the parameter modeling the linearity error. The bias and linearity errors are monitored and possibly eliminated by means of a gauge calibration, see the AIAG manual [6] for further details.

Let $\bar{X}^*_{i,j}$ denote the mean of m observed quantities of the same item j at the ith sampling. It is straightforward to show that

$$\bar{X}^*_{i,j} \sim N(\mu^*, \sigma^{*2}) = N\left(A + B(\mu_0 + a\sigma_0), B^2b^2\sigma_0^2 + \frac{\sigma_M^2}{m}\right).$$

Tran *et al.* [19] showed that the CV of the quantity $\bar{X}^*_{i,j}$ is

$$\gamma^* = \frac{\sigma^*}{\mu^*} = \frac{\sqrt{B^2b^2 + \frac{\eta^2}{m}}}{\theta + B(1 + a\gamma_0)} \times \gamma_0, \tag{15}$$

where $\gamma_0 = \sigma_0/\mu_0, \eta = \sigma_M/\sigma_0$ and $\theta = A/\mu_0$ are the in-control value of CV, the precision and the accuracy error ratios, respectively. The sample coefficient of variation $\hat{\gamma}^*_i$ is defined by $\hat{\gamma}^*_i = S^*_i/\bar{\bar{X}}^*_i$ where $\bar{\bar{X}}^*_i$ and S^*_i are the sample mean and standard deviation of $\bar{X}^*_{1,j}, \ldots, \bar{X}^*_{n,j}$ $\bar{X}^*_{1,j}, \ldots, \bar{X}^*_{n,j}$, i.e.

$$\bar{\bar{X}}^*_i = \frac{1}{n}\sum_{j=1}^{n} \bar{X}^*_{i,j} \quad \text{and} \quad S^*_i = \sqrt{\frac{1}{n-1}\sum_{j=1}^{n}(\bar{X}^*_{i,j} - \bar{\bar{X}}^*_i)^2}.$$

The *c.d.f* of $\hat{\gamma}^{*2}$ can be obtained from (2) by simply replacing γ by γ^*, i.e. the *c.d.f* $F_{\hat{\gamma}^{*2}}(x \mid n, \gamma^*)$ of $\hat{\gamma}^{*2}$ is given by

$$F_{\hat{\gamma}^{*2}}(x|n, \gamma^*) = 1 - F_F\left(\frac{n}{x}\middle|1, n-1, \frac{n}{\gamma^{*2}}\right). \tag{16}$$

6. Implementation and the performance of the $RR_{r,s} - \gamma^2$ charts with measurement errors

Under the presence of measurement errors, the values $\mu_0(\hat{\gamma}^{*2})$ and $\sigma_0(\hat{\gamma}^{*2})$ are calculated as in (4) and (5), where γ_0 is replaced by γ_0^*, which is defined from (15) with $a = 0$ and $b = 1$:

$$\gamma_0^* = \frac{\sqrt{B^2 + \frac{\eta^2}{m}}}{\theta + B} \times \gamma_0. \tag{17}$$

Suppose that the in-control value γ_0 is shifted to the out-of-control value γ_1 with the size τ, we can represent τ according to a and b as $\tau = b/(1 + a\gamma_0)$. Therefore, the out-of-control

CV of the observed quantity $\bar{X}^*_{i,j}$ can be expressed by

$$\gamma_1^* = \frac{\sqrt{B^2b^2 + \frac{\eta^2}{m}}}{\theta + \frac{Bb}{\tau}} \times \gamma_0. \tag{18}$$

In the implementation of $\mathrm{RR}_{r,s} - \gamma^2$ control charts, the control limits, $UCL^{*+} = \mu_0(\hat{\gamma}^{*2}) + k_u^*.\sigma_0(\hat{\gamma}^{*2})$ and $LCL^{*-} = \mu_0(\hat{\gamma}^{*2}) - k_d^*.\sigma_0(\hat{\gamma}^{*2})$, are also found by solving the chart parameters k_d and k_u as the solution of the following equations:

- for the $\mathrm{RR}^-_{r,s} - \gamma^2$ chart:

$$ARL(k_d, n, p, \gamma_0, \theta, \eta, m, B, b) = ARL_0, \tag{19}$$

- for the $\mathrm{RR}^+_{r,s} - \gamma^2$ chart:

$$ARL(k_u, n, p, \gamma_0, \theta, \eta, m, B, b) = ARL_0. \tag{20}$$

The *ARL* in (19) and (20) should be calculated with the transition probability matrix **Q** where the transition probability p is defined from (9) and (10) but with the *c.d.f* $F_{\hat{\gamma}^{*2}}(x \mid n, \gamma^*)$ of $\hat{\gamma}^{*2}$ in (16) instead of *c.d.f* $F_{\hat{\gamma}^2}$ in (2).

To investigate the performance of the $\mathrm{RR}_{r,s} - \gamma^2$ charts under the appearance of the measurement error, we consider several possible values of the parameters: $n \in \{5, 15\}$, $\gamma_0 \in \{0.05, 0.1, 0.2\}$, $\eta \in \{0, 0.1, 0.2, 0.3, 0.5, 1\}$, $\theta \in \{0, 0.01, 0.02, 0.03, 0.04, 0.05\}$, $m \in \{1, 3, 5, 7, 10\}$ and $B \in \{0.8, 0.9, 1, 1.1, 1.2\}$. The value of B is considered within the range $[0.8, 1.2]$ according to the guidelines for measurement system acceptability presented in manual of AIA Group [6] for measurement system analysis. Without loss of generality, we assume in the remaining that $b = 1$. The in-control value CV is also set at $ARL_0 = 370.4$.

The control limits of the proposed charts for some specific values of these parameters have been presented in Table 3. The other values of the control limits for other situations of these parameters are not presented here but are available upon request from authors.

Table 3. Values of *LCL* (first row) and *UCL* (second row) for the $\mathrm{RR}_{r,s} - \gamma^2$ control charts in the presence of measurement errors, for different values of $\eta, \theta, n, \gamma_0, B = 1$ and $m = 1$.

			$\mathrm{RR}_{2,3} - \gamma^2$		$\mathrm{RR}_{3,4} - \gamma^2$		$\mathrm{RR}_{3,4} - \gamma^2$	
η	θ	γ_0	$n = 10$	$n = 15$	$n = 10$	$n = 15$	$n = 10$	$n = 15$
0.1	0.01	0.05	0.0004	0.0011	0.0007	0.0014	0.0009	0.0016
			0.0063	0.0044	0.0047	0.0037	0.0039	0.0033
		0.10	0.0015	0.0043	0.0027	0.0055	0.0038	0.0065
			0.0254	0.0175	0.0191	0.0148	0.0156	0.0132
			0.0582	0.0399	0.0435	0.0336	0.0354	0.0299
		0.20	0.0059	0.0172	0.0107	0.0220	0.0151	0.0257
			0.1061	0.0718	0.0786	0.0602	0.0636	0.0534
0.28	0.05	0.05	0.0004	0.0011	0.0007	0.0014	0.0009	0.0016
			0.0062	0.0043	0.0047	0.0036	0.0038	0.0033
		0.10	0.0015	0.0043	0.0027	0.0055	0.0037	0.0064
			0.0251	0.0173	0.0189	0.0146	0.0154	0.0130
			0.0575	0.0394	0.0430	0.0332	0.0350	0.0295
		0.20	0.0059	0.0170	0.0106	0.0218	0.0149	0.0254
			0.1047	0.0709	0.0776	0.0595	0.0629	0.0528

Tables 4–7 show the corresponding values of the ARL_1 under different effects of the parameters η, θ, m and B of the linear covariate model. Some simple conclusions can be drawn from these tables as follows:

- The increase of the precision error ratio η leads to an increase of the ARL_1. However, this increase in the ARL_1 following the change of η is not significant, especially when $\eta \leqslant 0.3$. For example, for the $\text{RR}_{2,3} - \gamma^2$ chart with $n = 5, \gamma_0 = 0.05, B = 1, m = 1, \theta = 0.05$ and $\tau = 0.8$, we have $ARL_1 = 93.12$ when $\eta = 0.0$ and $ARL_1 = 93.20$ when $\eta = 0.3$ (Table 4). That means the precision error ratio does not affect much the performance of the proposed charts.
- The accuracy error θ has a negative impact on the $\text{RR}_{r,s} - \gamma^2$ charts' performance: the larger the accuracy error θ is, the larger the value ARL_1 is, i.e. the lower of the control chart is in detecting the out-of-control condition. For example, in the $\text{RR}_{3,4} - \gamma^2$ chart with $n = 5, \gamma_0 = 0.1, B = 1, m = 1, \eta = 0.28$ and $\tau = 1.3$, we have $ARL_1 = 26.56$ when $\theta = 0.0$ and $ARL_1 = 29.19$ when $\theta = 0.5$ (Table 5).
- Given the value of other parameters, the variation of B significantly affects the performance of the $\text{RR}_{r,s} - \gamma^2$ charts. For instance, in Table 6 with the $\text{RR}^{-}_{4,5} - \gamma^2$ control chart and $n = 5, m = 1, \gamma_0 = 0.2, \eta = 0.28, \theta = 0.05, \tau = 0.7$ we have $ARL_1 = 14.43$ when $B = 0.8$ and $ARL_1 = 13.93$ when $B = 1.2$.
- In many situations, taking multiple measurements per item in each sample is an alternative to compensate for the effect of the measurement error. However, the obtained results in this study show that this is not an effective way to reduce the impact of measurement errors on the proposed control charts performance. This is because, according to the results of the numerical analysis, the ARL_1 decreases trivially or is almost unchanged when m increases from $m = 1$ to $m = 10$. For example, with $n = 5, B = 1, \gamma_0 = 0.05, \eta = 0.28, \theta = 0.05, \tau = 0.8$ in the $\text{RR}^{+}_{2,3} - \gamma^2$, we have $ARL_1 = 9.07$ for both $m = 1$ and $m = 10$ (Table 7). Hence, in order to reduce the impact of ME on the proposed control charts performance, we can improve the measurement system to reduce the values of θ and η.
- In general, the $\text{RR}_{r,s} - \gamma^2$ control charts give better performance in detecting the small process shifts compared to the VSI-γ^2 control chart investigated in [11], under the same condition of measurement errors. For example, with the same values of $n = 5, \gamma_0 = 0.05, \eta = 0.28, \theta = 0.05, \tau = 0.8$, we have $ARL_1 = 46.80$ for the $\text{RR}_{4,5} - \gamma^2$ (Table 5 in this study), which is smaller than $ARL_1 = 61.99$ for the VSI γ^2 control chart with $(h_S, h_L) = 0.1, 4.0$ (Table 10 in [11]).

In practice, quality practitioners often prefer detecting a range of shifts $\Omega = [a; b]$ since it is difficult to guess an exact value for the process shift. In such situations, the statistical performance of the control chart can be evaluated through the *EARL* (expected average run length) defined as

$$EARL = \int_{\Omega} ARL \times f_{\tau}(\tau)\, \mathrm{d}\tau, \tag{21}$$

where $f_{\tau}(\tau)$ is the distribution of process shift τ and ARL is defined in (11). Without any information about τ, one can choose the uniform distribution in Ω, i.e $f_{\tau}(\tau) = 1/(b - a)$.

Table 4. The *ARL* values of the $RR_{r,s} - \gamma^2$ control charts in the presence of measurement errors for $\gamma_0 = 0.05$ (left side), $\gamma_0 = 0.1$ (middle) and $\gamma_0 = 0.2$ (right side), and for different values of $\eta, \theta = 0.05, \tau, n, B = 1, m = 1$.

Charts	τ	$\eta = 0$	$\eta = 0.1$	$\eta = 0.2$	$\eta = 0.3$	$\eta = 0.5$	$\eta = 1$
				$n = 5$			
$RR_{2,3} - \gamma^2$	0.5	(8.92, 8.85, 8.98)	(8.94, 8.85, 8.99)	(8.92, 8.84, 8.99)	(8.92, 8.86, 9.01)	(8.90, 8.84, 9.06)	(8.87, 8.87, 9.24)
	0.7	(29.38, 29.11, 29.54)	(29.45, 29.14, 29.58)	(29.35, 29.06, 29.57)	(29.40, 29.13, 29.65)	(29.29, 29.09, 29.80)	(29.19, 29.18, 30.42)
	0.8	(93.12, 92.52, 93.41)	(93.28, 92.44, 93.58)	(93.15, 92.24, 93.38)	(93.20, 92.54, 93.68)	(92.90, 92.39, 93.98)	(92.74, 92.60, 95.22)
	1.3	(28.57, 28.83, 29.93)	(28.57, 28.84, 29.94)	(28.57, 28.85, 29.99)	(28.58, 28.87, 30.06)	(28.59, 28.92, 30.30)	(28.66, 29.19, 31.45)
	1.5	(9.07, 9.17, 9.62)	(9.07, 9.17, 9.62)	(9.07, 9.18, 9.64)	(9.07, 9.19, 9.67)	(9.07, 9.21, 9.77)	(9.10, 9.32, 10.24)
	2.0	(3.70, 3.74, 3.92)	(3.70, 3.74, 3.92)	(3.70, 3.74, 3.92)	(3.70, 3.75, 3.94)	(3.70, 3.76, 3.98)	(3.71, 3.80, 4.16)
$RR_{3,4} - \gamma^2$	0.5	(6.01, 6.02, 6.11)	(6.02, 6.02, 6.12)	(6.02, 6.02, 6.12)	(6.01, 6.02, 6.13)	(6.01, 6.02, 6.15)	(6.01, 6.05, 6.26)
	0.7	(17.69, 17.71, 18.09)	(17.71, 17.71, 18.11)	(17.71, 17.71, 18.11)	(17.70, 17.73, 18.15)	(17.71, 17.73, 18.25)	(17.68, 17.82, 18.68)
	0.8	(64.10, 64.21, 65.33)	(64.20, 64.19, 65.35)	(64.22, 64.17, 65.37)	(64.13, 64.24, 65.47)	(64.22, 64.25, 65.78)	(64.07, 64.48, 67.06)
	1.3	(28.92, 29.17, 30.21)	(28.92, 29.17, 30.22)	(28.92, 29.18, 30.26)	(28.93, 29.20, 30.34)	(28.93, 29.25, 30.56)	(29.00, 29.51, 31.63)
	1.5	(10.01, 10.12, 10.55)	(10.01, 10.12, 10.55)	(10.01, 10.12, 10.57)	(10.02, 10.13, 10.60)	(10.02, 10.15, 10.69)	(10.05, 10.26, 11.14)
	2.0	(4.67, 4.71, 4.89)	(4.67, 4.71, 4.89)	(4.67, 4.72, 4.90)	(4.67, 4.72, 4.91)	(4.68, 4.73, 4.95)	(4.69, 4.77, 5.13)
$RR_{4,5} - \gamma^2$	0.5	(5.64, 5.65, 5.71)	(5.64, 5.65, 5.71)	(5.64, 5.65, 5.72)	(5.64, 5.65, 5.72)	(5.64, 5.65, 5.74)	(5.64, 5.67, 5.81)
	0.7	(13.75, 13.79, 14.09)	(13.76, 13.80, 14.10)	(13.76, 13.81, 14.12)	(13.75, 13.81, 14.13)	(13.76, 13.81, 14.20)	(13.76, 13.89, 14.52)
	0.8	(50.44, 50.60, 51.63)	(50.49, 50.63, 51.67)	(50.51, 50.66, 51.74)	(50.45, 50.66, 51.78)	(50.46, 50.67, 52.03)	(50.48, 50.96, 53.14)
	1.3	(30.17, 30.42, 31.45)	(30.18, 30.43, 31.46)	(30.19, 30.43, 31.51)	(30.18, 30.45, 31.57)	(30.20, 30.51, 31.80)	(30.25, 30.76, 32.85)
	1.5	(11.17, 11.27, 11.70)	(11.17, 11.27, 11.71)	(11.17, 11.27, 11.73)	(11.17, 11.28, 11.76)	(11.17, 11.30, 11.85)	(11.20, 11.41, 12.30)
	2.0	(5.68, 5.72, 5.90)	(5.68, 5.72, 5.90)	(5.68, 5.72, 5.91)	(5.68, 5.72, 5.92)	(5.68, 5.73, 5.96)	(5.69, 5.78, 6.14)
				$n = 15$			
$RR_{2,3} - \gamma^2$	0.5	(2.12, 2.12, 2.13)	(2.12, 2.12, 2.13)	(2.12, 2.12, 2.13)	(2.12, 2.12, 2.13)	(2.12, 2.12, 2.14)	(2.12, 2.12, 2.15)
	0.7	(4.12, 4.08, 4.18)	(4.12, 4.08, 4.18)	(4.12, 4.08, 4.18)	(4.11, 4.08, 4.19)	(4.11, 4.08, 4.22)	(4.09, 4.10, 4.35)
	0.8	(19.86, 19.42, 19.97)	(19.83, 19.43, 20.02)	(19.83, 19.45, 20.02)	(19.80, 19.45, 20.06)	(19.73, 19.43, 20.20)	(19.56, 19.55, 21.01)
	1.3	(9.68, 9.81, 10.41)	(9.68, 9.82, 10.41)	(9.68, 9.82, 10.44)	(9.68, 9.83, 10.48)	(9.69, 9.86, 10.61)	(9.72, 10.01, 11.22)
	1.5	(3.32, 3.36, 3.52)	(3.32, 3.36, 3.52)	(3.32, 3.36, 3.53)	(3.32, 3.36, 3.54)	(3.32, 3.37, 3.58)	(3.33, 3.41, 3.75)
	2.0	(2.13, 2.14, 2.17)	(2.13, 2.14, 2.17)	(2.13, 2.14, 2.18)	(2.13, 2.14, 2.18)	(2.13, 2.14, 2.19)	(2.13, 2.15, 2.23)

$RR_{3,4} - \gamma^2$	0.5	(3.02, 3.02, 3.03)	(3.02, 3.02, 3.03)	(3.02, 3.02, 3.03)	(3.02, 3.02, 3.03)	(3.02, 3.02, 3.03)	(3.02, 3.03, 3.03)
	0.7	(4.02, 4.02, 4.09)	(4.02, 4.02, 4.09)	(4.01, 4.02, 4.10)	(4.01, 4.02, 4.10)	(4.01, 4.03, 4.12)	(4.01, 4.04, 4.20)
	0.8	(13.91, 13.92, 14.41)	(13.92, 13.91, 14.42)	(13.90, 13.91, 14.44)	(13.90, 13.92, 14.48)	(13.89, 13.95, 14.59)	(13.87, 14.06, 15.13)
	1.3	(9.77, 9.89, 10.42)	(9.77, 9.90, 10.42)	(9.78, 9.90, 10.44)	(9.78, 9.91, 10.48)	(9.78, 9.94, 10.59)	(9.81, 10.07, 11.13)
	1.5	(4.10, 4.13, 4.28)	(4.10, 4.13, 4.28)	(4.10, 4.14, 4.29)	(4.10, 4.14, 4.30)	(4.10, 4.14, 4.33)	(4.11, 4.18, 4.48)
	2.0	(3.09, 3.10, 3.12)	(3.09, 3.10, 3.13)	(3.09, 3.10, 3.13)	(3.09, 3.10, 3.13)	(3.09, 3.10, 3.14)	(3.09, 3.11, 3.17)
$RR_{4,5} - \gamma^2$	0.5	(4.01, 4.01, 4.01)	(4.01, 4.01, 4.01)	(4.01, 4.01, 4.01)	(4.01, 4.01, 4.01)	(4.01, 4.01, 4.01)	(4.01, 4.01, 4.01)
	0.7	(4.58, 4.59, 4.64)	(4.58, 4.59, 4.64)	(4.58, 4.59, 4.64)	(4.58, 4.59, 4.65)	(4.58, 4.59, 4.66)	(4.58, 4.60, 4.71)
	0.8	(12.09, 12.14, 12.55)	(12.09, 12.14, 12.56)	(12.09, 12.14, 12.58)	(12.09, 12.15, 12.61)	(12.09, 12.17, 12.70)	(12.09, 12.27, 13.15)
	1.3	(10.37, 10.48, 10.97)	(10.37, 10.48, 10.98)	(10.37, 10.49, 11.00)	(10.37, 10.49, 11.03)	(10.38, 10.52, 11.14)	(10.40, 10.64, 11.64)
	1.5	(4.97, 5.00, 5.13)	(4.97, 5.00, 5.13)	(4.97, 5.00, 5.14)	(4.97, 5.00, 5.15)	(4.97, 5.01, 5.18)	(4.98, 5.04, 5.32)
	2.0	(4.07, 4.08, 4.10)	(4.07, 4.08, 4.10)	(4.07, 4.08, 4.10)	(4.07, 4.08, 4.10)	(4.07, 4.08, 4.11)	(4.07, 4.08, 4.13)

Table 5. The *ARL* values of the $RR_{r,s} - \gamma^2$ control charts in the presence of measurement errors for $\gamma_0 = 0.05$ (left side), $\gamma_0 = 0.1$ (middle) and $\gamma_0 = 0.2$ (right side), and for different values of θ, $\eta = 0.28$, τ, $n, B = 1, m = 1$.

Charts	τ	$\theta = 0$	$\theta = 0.01$	$\theta = 0.02$	$\theta = 0.03$	$\theta = 0.04$	$\theta = 0.05$
				$n = 5$			
$RR_{2,3} - \gamma^2$	0.5	(8.11, 8.06, 8.22)	(8.28, 8.21, 8.38)	(8.43, 8.35, 8.53)	(8.59, 8.52, 8.69)	(8.75, 8.69, 8.84)	(8.93, 8.85, 9.01)
	0.7	(26.88, 26.65, 27.19)	(27.38, 27.15, 27.71)	(27.87, 27.55, 28.15)	(28.36, 28.10, 28.66)	(28.87, 28.62, 29.12)	(29.42, 29.13, 29.64)
	0.8	(87.72, 87.23, 88.36)	(88.96, 88.30, 89.56)	(89.94, 89.12, 90.51)	(90.85, 90.33, 91.69)	(91.95, 91.30, 92.44)	(93.24, 92.53, 93.63)
	1.3	(25.84, 26.13, 27.35)	(26.38, 26.67, 27.88)	(26.93, 27.21, 28.42)	(27.47, 27.76, 28.96)	(28.02, 28.31, 29.50)	(28.58, 28.86, 30.04)
	1.5	(8.09, 8.20, 8.68)	(8.28, 8.39, 8.87)	(8.47, 8.59, 9.07)	(8.67, 8.78, 9.26)	(8.87, 8.98, 9.46)	(9.07, 9.18, 9.66)
	2.0	(3.38, 3.42, 3.61)	(3.44, 3.48, 3.67)	(3.50, 3.55, 3.73)	(3.57, 3.61, 3.80)	(3.63, 3.68, 3.87)	(3.70, 3.75, 3.93)
$RR_{3,4} - \gamma^2$	0.5	(5.60, 5.61, 5.71)	(5.68, 5.69, 5.80)	(5.76, 5.77, 5.88)	(5.84, 5.85, 5.96)	(5.93, 5.93, 6.04)	(6.01, 6.02, 6.12)
	0.7	(16.15, 16.20, 16.62)	(16.47, 16.50, 16.93)	(16.76, 16.78, 17.24)	(17.07, 17.10, 17.53)	(17.38, 17.40, 17.84)	(17.70, 17.72, 18.14)
	0.8	(59.75, 59.92, 61.22)	(60.70, 60.79, 62.12)	(61.56, 61.53, 63.02)	(62.38, 62.49, 63.79)	(63.26, 63.35, 64.67)	(64.20, 64.24, 65.45)
	1.3	(26.28, 26.56, 27.72)	(26.80, 27.08, 28.23)	(27.33, 27.60, 28.75)	(27.86, 28.13, 29.27)	(28.39, 28.66, 29.79)	(28.92, 29.19, 30.31)
	1.5	(9.05, 9.16, 9.63)	(9.24, 9.35, 9.82)	(9.43, 9.54, 10.01)	(9.62, 9.73, 10.20)	(9.82, 9.93, 10.39)	(10.02, 10.13, 10.59)
	2.0	(4.35, 4.39, 4.58)	(4.41, 4.46, 4.64)	(4.48, 4.52, 4.70)	(4.54, 4.58, 4.77)	(4.61, 4.65, 4.84)	(4.67, 4.72, 4.91)
$RR_{4,5} - \gamma^2$	0.5	(5.37, 5.39, 5.46)	(5.43, 5.44, 5.51)	(5.48, 5.49, 5.56)	(5.53, 5.54, 5.61)	(5.58, 5.59, 5.67)	(5.64, 5.65, 5.72)
	0.7	(12.65, 12.70, 13.04)	(12.87, 12.92, 13.25)	(13.09, 13.14, 13.47)	(13.31, 13.35, 13.68)	(13.53, 13.58, 13.90)	(13.76, 13.80, 14.13)
	0.8	(46.80, 47.00, 48.23)	(47.56, 47.75, 48.90)	(48.26, 48.47, 49.65)	(49.00, 49.14, 50.35)	(49.70, 49.91, 51.07)	(50.47, 50.63, 51.74)
	1.3	(27.55, 27.82, 28.97)	(28.07, 28.34, 29.48)	(28.60, 28.86, 29.99)	(29.13, 29.39, 30.51)	(29.65, 29.92, 31.04)	(30.19, 30.44, 31.56)
	1.5	(10.18, 10.30, 10.77)	(10.38, 10.49, 10.96)	(10.57, 10.68, 11.15)	(10.77, 10.88, 11.35)	(10.97, 11.08, 11.55)	(11.17, 11.28, 11.75)
	2.0	(5.34, 5.39, 5.58)	(5.41, 5.45, 5.64)	(5.47, 5.52, 5.71)	(5.54, 5.58, 5.77)	(5.61, 5.65, 5.84)	(5.68, 5.72, 5.91)
				$n = 15$			
$RR_{2,3} - \gamma^2$	0.5	(2.09, 2.09, 2.10)	(2.09, 2.09, 2.10)	(2.10, 2.10, 2.11)	(2.11, 2.11, 2.12)	(2.11, 2.11, 2.13)	(2.12, 2.12, 2.13)
	0.7	(3.79, 3.76, 3.87)	(3.85, 3.82, 3.94)	(3.92, 3.89, 4.00)	(3.98, 3.95, 4.06)	(4.04, 4.02, 4.12)	(4.12, 4.08, 4.19)
	0.8	(17.85, 17.59, 18.24)	(18.22, 17.94, 18.60)	(18.65, 18.32, 18.96)	(19.00, 18.68, 19.31)	(19.39, 19.08, 19.68)	(19.82, 19.40, 20.05)
	1.3	(8.66, 8.81, 9.44)	(8.86, 9.01, 9.64)	(9.06, 9.21, 9.84)	(9.26, 9.41, 10.05)	(9.47, 9.62, 10.26)	(9.68, 9.83, 10.47)
	1.5	(3.07, 3.11, 3.28)	(3.12, 3.16, 3.33)	(3.17, 3.21, 3.38)	(3.22, 3.26, 3.43)	(3.27, 3.31, 3.48)	(3.32, 3.36, 3.54)

	2.0	(2.08, 2.09, 2.13)	(2.09, 2.10, 2.14)	(2.10, 2.11, 2.15)	(2.11, 2.12, 2.16)	(2.12, 2.13, 2.17)	(2.13, 2.14, 2.18)
$RR_{3,4} - \gamma^2$	0.5	(3.01, 3.02, 3.02)	(3.02, 3.02, 3.02)	(3.02, 3.02, 3.02)	(3.02, 3.02, 3.02)	(3.02, 3.02, 3.03)	(3.02, 3.02, 3.03)
	0.7	(3.83, 3.84, 3.91)	(3.87, 3.87, 3.95)	(3.90, 3.91, 3.99)	(3.94, 3.95, 4.02)	(3.98, 3.98, 4.06)	(4.02, 4.02, 4.10)
	0.8	(12.64, 12.68, 13.22)	(12.89, 12.92, 13.47)	(13.14, 13.16, 13.71)	(13.38, 13.41, 13.97)	(13.64, 13.67, 14.22)	(13.91, 13.92, 14.46)
	1.3	(8.87, 9.00, 9.56)	(9.04, 9.18, 9.74)	(9.22, 9.36, 9.92)	(9.41, 9.54, 10.10)	(9.59, 9.72, 10.28)	(9.78, 9.91, 10.47)
	1.5	(3.88, 3.91, 4.06)	(3.92, 3.96, 4.11)	(3.97, 4.00, 4.15)	(4.01, 4.04, 4.20)	(4.06, 4.09, 4.25)	(4.10, 4.14, 4.29)
	2.0	(3.06, 3.06, 3.09)	(3.07, 3.07, 3.10)	(3.07, 3.08, 3.10)	(3.08, 3.08, 3.11)	(3.09, 3.09, 3.12)	(3.09, 3.10, 3.13)
$RR_{4,5} - \gamma^2$	0.5	(4.00, 4.00, 4.00)	(4.00, 4.00, 4.01)	(4.00, 4.00, 4.01)	(4.01, 4.01, 4.01)	(4.01, 4.01, 4.01)	(4.01, 4.01, 4.01)
	0.7	(4.46, 4.47, 4.52)	(4.48, 4.49, 4.54)	(4.51, 4.51, 4.57)	(4.53, 4.54, 4.59)	(4.55, 4.56, 4.62)	(4.58, 4.59, 4.64)
	0.8	(11.10, 11.17, 11.62)	(11.29, 11.36, 11.82)	(11.48, 11.55, 12.01)	(11.69, 11.75, 12.21)	(11.89, 11.94, 12.40)	(12.09, 12.14, 12.60)
	1.3	(9.50, 9.63, 10.15)	(9.67, 9.79, 10.32)	(9.84, 9.97, 10.49)	(10.02, 10.14, 10.67)	(10.19, 10.31, 10.85)	(10.37, 10.49, 11.02)
	1.5	(4.77, 4.80, 4.93)	(4.81, 4.84, 4.97)	(4.85, 4.88, 5.02)	(4.89, 4.92, 5.06)	(4.93, 4.96, 5.10)	(4.97, 5.00, 5.15)
	2.0	(4.05, 4.05, 4.07)	(4.05, 4.05, 4.07)	(4.06, 4.06, 4.08)	(4.06, 4.06, 4.09)	(4.07, 4.07, 4.09)	(4.07, 4.08, 4.10)

Table 6. The *ARL* values of the $RR_{r,s} - \gamma^2$ control charts in the presence of measurement errors for $\gamma_0 = 0.05$ (left side), $\gamma_0 = 0.1$ (middle) and $\gamma_0 = 0.2$ (right side), and for different values of $B, \tau, n, \eta = 0.28, \theta = 0.05, m = 1$.

Charts	τ	$B = 0.8$	$B = 0.9$	$B = 1.0$	$B = 1.1$	$B = 1.2$
				$n = 5$		
$RR_{2,3} - \gamma^2$	0.5	(9.13, 9.05, 9.22)	(9.03, 8.93, 9.11)	(8.93, 8.85, 9.01)	(8.84, 8.76, 8.94)	(8.79, 8.72, 8.87)
	0.7	(30.00, 29.74, 30.26)	(29.73, 29.33, 29.95)	(29.42, 29.13, 29.64)	(29.10, 28.82, 29.42)	(28.99, 28.71, 29.24)
	0.8	(94.27, 93.68, 94.95)	(93.89, 92.84, 94.31)	(93.24, 92.53, 93.63)	(92.45, 91.72, 93.28)	(92.23, 91.63, 92.81)
	1.3	(29.28, 29.57, 30.79)	(28.89, 29.17, 30.37)	(28.58, 28.86, 30.04)	(28.33, 28.60, 29.77)	(28.11, 28.39, 29.55)
	1.5	(9.33, 9.44, 9.95)	(9.18, 9.30, 9.79)	(9.07, 9.18, 9.66)	(8.98, 9.09, 9.56)	(8.90, 9.01, 9.48)
	2.0	(3.79, 3.83, 4.03)	(3.74, 3.78, 3.98)	(3.70, 3.75, 3.93)	(3.67, 3.71, 3.90)	(3.64, 3.69, 3.87)
$RR_{3,4} - \gamma^2$	0.5	(6.12, 6.13, 6.24)	(6.06, 6.06, 6.18)	(6.01, 6.02, 6.12)	(5.98, 5.98, 6.09)	(5.94, 5.95, 6.05)
	0.7	(18.08, 18.11, 18.55)	(17.89, 17.88, 18.33)	(17.70, 17.72, 18.14)	(17.57, 17.58, 18.00)	(17.44, 17.46, 17.88)
	0.8	(65.22, 65.28, 66.56)	(64.70, 64.64, 66.01)	(64.20, 64.24, 65.45)	(63.85, 63.84, 65.08)	(63.43, 63.53, 64.76)
	1.3	(29.60, 29.88, 31.04)	(29.22, 29.50, 30.63)	(28.92, 29.19, 30.31)	(28.68, 28.94, 30.06)	(28.48, 28.74, 29.84)
	1.5	(10.27, 10.38, 10.87)	(10.13, 10.24, 10.71)	(10.02, 10.13, 10.59)	(9.93, 10.03, 10.49)	(9.85, 9.96, 10.41)
	2.0	(4.76, 4.81, 5.00)	(4.71, 4.76, 4.95)	(4.67, 4.72, 4.91)	(4.64, 4.69, 4.87)	(4.62, 4.66, 4.84)
$RR_{4,5} - \gamma^2$	0.5	(5.71, 5.72, 5.79)	(5.67, 5.68, 5.75)	(5.64, 5.65, 5.72)	(5.61, 5.62, 5.69)	(5.59, 5.60, 5.67)
	0.7	(14.04, 14.08, 14.43)	(13.88, 13.93, 14.26)	(13.76, 13.80, 14.13)	(13.66, 13.70, 14.02)	(13.57, 13.61, 13.93)
	0.8	(51.38, 51.54, 52.76)	(50.91, 51.07, 52.19)	(50.47, 50.63, 51.74)	(50.18, 50.32, 51.43)	(49.86, 50.02, 51.15)
	1.3	(30.85, 31.13, 32.28)	(30.48, 30.75, 31.88)	(30.19, 30.44, 31.56)	(29.94, 30.20, 31.30)	(29.74, 30.00, 31.09)
	1.5	(11.42, 11.54, 12.03)	(11.28, 11.40, 11.87)	(11.17, 11.28, 11.75)	(11.08, 11.19, 11.65)	(11.00, 11.11, 11.57)
	2.0	(5.77, 5.81, 6.01)	(5.72, 5.76, 5.96)	(5.68, 5.72, 5.91)	(5.65, 5.69, 5.88)	(5.62, 5.66, 5.85)
				$n = 15$		
$RR_{2,3} - \gamma^2$	0.5	(2.13, 2.13, 2.14)	(2.13, 2.13, 2.14)	(2.12, 2.12, 2.13)	(2.12, 2.12, 2.13)	(2.12, 2.11, 2.13)
	0.7	(4.20, 4.17, 4.29)	(4.15, 4.12, 4.23)	(4.12, 4.08, 4.19)	(4.08, 4.05, 4.16)	(4.06, 4.02, 4.13)
	0.8	(20.29, 19.95, 20.61)	(20.05, 19.69, 20.26)	(19.82, 19.40, 20.05)	(19.64, 19.25, 19.86)	(19.50, 19.11, 19.73)

	1.3	(9.95, 10.11, 10.77)	(9.80, 9.95, 10.60)	(9.68, 9.83, 10.47)	(9.58, 9.73, 10.36)	(9.50, 9.65, 10.28)
	1.5	(3.39, 3.43, 3.62)	(3.35, 3.39, 3.57)	(3.32, 3.36, 3.54)	(3.30, 3.34, 3.51)	(3.28, 3.31, 3.49)
	2.0	(2.14, 2.15, 2.19)	(2.13, 2.14, 2.18)	(2.13, 2.14, 2.18)	(2.12, 2.13, 2.17)	(2.12, 2.13, 2.17)
$RR_{3,4} - \gamma^2$	0.5	(3.03, 3.03, 3.03)	(3.03, 3.03, 3.03)	(3.02, 3.02, 3.03)	(3.02, 3.02, 3.03)	(3.02, 3.02, 3.03)
	0.7	(4.06, 4.07, 4.15)	(4.04, 4.04, 4.12)	(4.02, 4.02, 4.10)	(4.00, 4.00, 4.08)	(3.98, 3.99, 4.06)
	0.8	(14.22, 14.25, 14.82)	(14.05, 14.07, 14.62)	(13.91, 13.92, 14.46)	(13.78, 13.81, 14.34)	(13.68, 13.71, 14.23)
	1.3	(10.02, 10.15, 10.74)	(9.88, 10.02, 10.59)	(9.78, 9.91, 10.47)	(9.69, 9.82, 10.38)	(9.62, 9.75, 10.30)
	1.5	(4.16, 4.20, 4.36)	(4.13, 4.16, 4.32)	(4.10, 4.14, 4.29)	(4.08, 4.12, 4.27)	(4.06, 4.10, 4.25)
	2.0	(3.10, 3.11, 3.14)	(3.10, 3.10, 3.13)	(3.09, 3.10, 3.13)	(3.09, 3.09, 3.12)	(3.09, 3.09, 3.12)
$RR_{4,5} - \gamma^2$	0.5	(4.01, 4.01, 4.01)	(4.01, 4.01, 4.01)	(4.01, 4.01, 4.01)	(4.01, 4.01, 4.01)	(4.01, 4.01, 4.01)
	0.7	(4.61, 4.62, 4.68)	(4.59, 4.60, 4.66)	(4.58, 4.59, 4.64)	(4.57, 4.58, 4.63)	(4.56, 4.57, 4.62)
	0.8	(12.34, 12.40, 12.88)	(12.20, 12.26, 12.72)	(12.09, 12.14, 12.60)	(12.00, 12.05, 12.50)	(11.92, 11.98, 12.42)
	1.3	(10.60, 10.72, 11.28)	(10.47, 10.60, 11.14)	(10.37, 10.49, 11.02)	(10.29, 10.41, 10.93)	(10.22, 10.34, 10.86)
	1.5	(5.03, 5.06, 5.21)	(5.00, 5.03, 5.18)	(4.97, 5.00, 5.15)	(4.95, 4.98, 5.12)	(4.94, 4.97, 5.11)
	2.0	(4.08, 4.08, 4.11)	(4.08, 4.08, 4.11)	(4.07, 4.08, 4.10)	(4.07, 4.07, 4.10)	(4.07, 4.07, 4.09)

Table 7. The *ARL* values of the $RR_{r,s} - \gamma^2$ control charts in the presence of measurement errors for $\gamma_0 = 0.05$ (left side), $\gamma_0 = 0.1$ (middle) and $\gamma_0 = 0.2$ (right side), and for different values of m, τ, n, $\eta = 0.28$, $\theta = 0.05$, $B = 1$.

Charts	τ	$m = 1$	$m = 3$	$m = 5$	$m = 7$	$m = 10$
				$n = 5$		
$RR_{2,3} - \gamma^2$	0.5	(8.93, 8.85, 9.01)	(8.92, 8.84, 8.99)	(8.93, 8.84, 8.99)	(8.94, 8.85, 8.99)	(8.93, 8.84, 8.99)
	0.7	(29.42, 29.13, 29.64)	(29.39, 29.06, 29.56)	(29.41, 29.09, 29.56)	(29.42, 29.11, 29.58)	(29.39, 29.07, 29.58)
	0.8	(93.24, 92.53, 93.63)	(93.00, 92.20, 93.47)	(93.22, 92.44, 93.43)	(93.20, 92.50, 93.57)	(93.12, 92.23, 93.52)
	1.3	(28.58, 28.86, 30.04)	(28.57, 28.84, 29.96)	(28.57, 28.84, 29.95)	(28.57, 28.83, 29.95)	(28.57, 28.83, 29.94)
	1.5	(9.07, 9.18, 9.66)	(9.07, 9.18, 9.63)	(9.07, 9.17, 9.62)	(9.07, 9.17, 9.62)	(9.07, 9.17, 9.62)
	2.0	(3.70, 3.75, 3.93)	(3.70, 3.74, 3.92)	(3.70, 3.74, 3.92)	(3.70, 3.74, 3.92)	(3.70, 3.74, 3.92)
$RR_{3,4} - \gamma^2$	0.5	(6.01, 6.02, 6.12)	(6.02, 6.02, 6.12)	(6.01, 6.01, 6.12)	(6.02, 6.02, 6.12)	(6.01, 6.02, 6.12)
	0.7	(17.70, 17.72, 18.14)	(17.72, 17.70, 18.11)	(17.70, 17.69, 18.11)	(17.71, 17.71, 18.10)	(17.69, 17.71, 18.11)
	0.8	(64.20, 64.24, 65.45)	(64.26, 64.15, 65.33)	(64.18, 64.15, 65.36)	(64.18, 64.21, 65.35)	(64.15, 64.15, 65.39)
	1.3	(28.92, 29.19, 30.31)	(28.92, 29.17, 30.25)	(28.92, 29.17, 30.23)	(28.92, 29.17, 30.22)	(28.92, 29.17, 30.22)
	1.5	(10.02, 10.13, 10.59)	(10.01, 10.12, 10.56)	(10.01, 10.12, 10.55)	(10.01, 10.12, 10.55)	(10.01, 10.12, 10.55)
	2.0	(4.67, 4.72, 4.91)	(4.67, 4.72, 4.89)	(4.67, 4.71, 4.89)	(4.67, 4.71, 4.89)	(4.67, 4.71, 4.89)
$RR_{4,5} - \gamma^2$	0.5	(5.64, 5.65, 5.72)	(5.64, 5.65, 5.71)	(5.64, 5.65, 5.71)	(5.64, 5.65, 5.71)	(5.64, 5.65, 5.71)
	0.7	(13.76, 13.80, 14.13)	(13.76, 13.80, 14.10)	(13.75, 13.80, 14.10)	(13.76, 13.79, 14.10)	(13.75, 13.79, 14.10)
	0.8	(50.47, 50.63, 51.74)	(50.50, 50.65, 51.67)	(50.46, 50.62, 51.68)	(50.48, 50.58, 51.67)	(50.47, 50.60, 51.67)
	1.3	(30.19, 30.44, 31.56)	(30.18, 30.43, 31.49)	(30.18, 30.43, 31.47)	(30.18, 30.42, 31.46)	(30.17, 30.42, 31.46)
	1.5	(11.17, 11.28, 11.75)	(11.17, 11.27, 11.72)	(11.17, 11.27, 11.71)	(11.17, 11.27, 11.71)	(11.17, 11.27, 11.71)
	2.0	(5.68, 5.72, 5.91)	(5.68, 5.72, 5.90)	(5.68, 5.72, 5.90)	(5.68, 5.72, 5.90)	(5.68, 5.72, 5.90)
				$n = 15$		
$RR_{2,3} - \gamma^2$	0.5	(2.12, 2.12, 2.13)	(2.12, 2.12, 2.13)	(2.12, 2.12, 2.13)	(2.12, 2.12, 2.13)	(2.12, 2.12, 2.13)
	0.7	(4.12, 4.08, 4.19)	(4.12, 4.08, 4.18)	(4.12, 4.08, 4.18)	(4.12, 4.08, 4.18)	(4.12, 4.08, 4.18)
	0.8	(19.82, 19.40, 20.05)	(19.83, 19.41, 19.99)	(19.86, 19.45, 20.00)	(19.85, 19.45, 20.00)	(19.84, 19.43, 19.98)
	1.3	(9.68, 9.83, 10.47)	(9.68, 9.82, 10.43)	(9.68, 9.82, 10.42)	(9.68, 9.82, 10.42)	(9.68, 9.82, 10.41)
	1.5	(3.32, 3.36, 3.54)	(3.32, 3.36, 3.53)	(3.32, 3.36, 3.52)	(3.32, 3.36, 3.52)	(3.32, 3.36, 3.52)

	2.0	(2.13, 2.14, 2.18)	(2.13, 2.14, 2.17)	(2.13, 2.14, 2.17)	(2.13, 2.14, 2.17)	(2.13, 2.14, 2.17)
$RR_{3,4} - \gamma^2$	0.5	(3.02, 3.02, 3.03)	(3.02, 3.02, 3.03)	(3.02, 3.02, 3.03)	(3.02, 3.02, 3.03)	(3.02, 3.02, 3.03)
	0.7	(4.02, 4.02, 4.10)	(4.02, 4.02, 4.10)	(4.01, 4.02, 4.09)	(4.02, 4.02, 4.09)	(4.01, 4.02, 4.09)
	0.8	(13.91, 13.92, 14.46)	(13.90, 13.92, 14.44)	(13.90, 13.91, 14.42)	(13.92, 13.90, 14.42)	(13.91, 13.90, 14.42)
	1.3	(9.78, 9.91, 10.47)	(9.78, 9.90, 10.44)	(9.78, 9.90, 10.43)	(9.78, 9.90, 10.42)	(9.78, 9.90, 10.42)
	1.5	(4.10, 4.14, 4.29)	(4.10, 4.13, 4.28)	(4.10, 4.13, 4.28)	(4.10, 4.13, 4.28)	(4.10, 4.13, 4.28)
	2.0	(3.09, 3.10, 3.13)	(3.09, 3.10, 3.13)	(3.09, 3.10, 3.13)	(3.09, 3.10, 3.13)	(3.09, 3.10, 3.13)
$RR_{4,5} - \gamma^2$	0.5	(4.01, 4.01, 4.01)	(4.01, 4.01, 4.01)	(4.01, 4.01, 4.01)	(4.01, 4.01, 4.01)	(4.01, 4.01, 4.01)
	0.7	(4.58, 4.59, 4.64)	(4.58, 4.59, 4.64)	(4.58, 4.59, 4.64)	(4.58, 4.59, 4.64)	(4.58, 4.59, 4.64)
	0.8	(12.09, 12.14, 12.60)	(12.09, 12.14, 12.57)	(12.09, 12.14, 12.57)	(12.09, 12.14, 12.56)	(12.09, 12.14, 12.56)
	1.3	(10.37, 10.49, 11.02)	(10.37, 10.48, 10.99)	(10.37, 10.48, 10.98)	(10.37, 10.48, 10.98)	(10.37, 10.48, 10.98)
	1.5	(4.97, 5.00, 5.15)	(4.97, 5.00, 5.14)	(4.97, 5.00, 5.14)	(4.97, 5.00, 5.13)	(4.97, 5.00, 5.13)
	2.0	(4.07, 4.08, 4.10)	(4.07, 4.08, 4.10)	(4.07, 4.08, 4.10)	(4.07, 4.08, 4.10)	(4.07, 4.08, 4.10)

The chart parameters are now defined as

- for the $\mathrm{RR}^{-}_{r,s} - \gamma^2$ chart:

$$EARL(LCL^{*-}, n, p, \gamma_0, \theta, \eta, m, B) = ARL_0, \tag{22}$$

- for the $\mathrm{RR}^{+}_{r,s} - \gamma^2$ chart:

$$EARL(UCL^{*+}, n, p, \gamma_0, \theta, \eta, m, B) = ARL_0. \tag{23}$$

In the following simulation, we consider a specific range of decreasing shifts $\Omega_D = [0.5, 1)$ and increasing shifts $\Omega_I = (1, 2]$. Figures 2 and 3 show the change of *EARL* of the

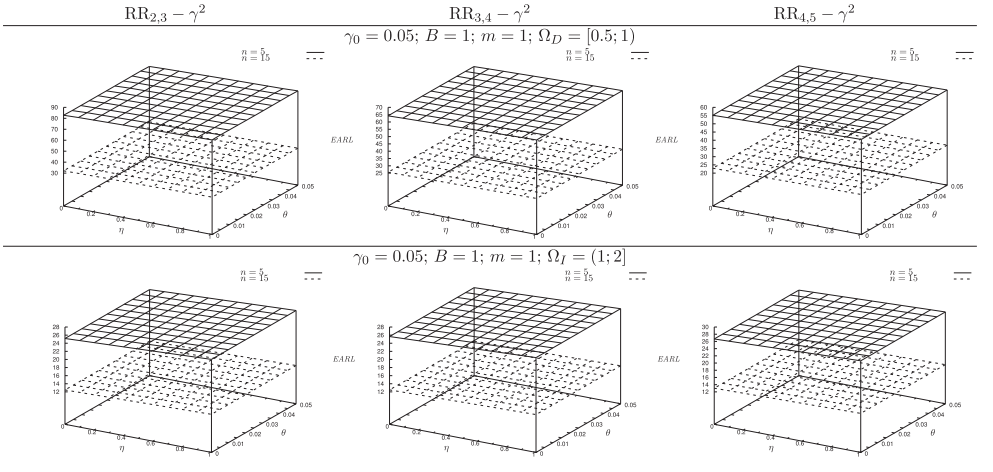

Figure 2. The effect of θ and η on the performance of the $\mathrm{RR}_{r,s} - \gamma^2$ control charts in the presence of measurement errors for $\gamma_0 = 0.05$.

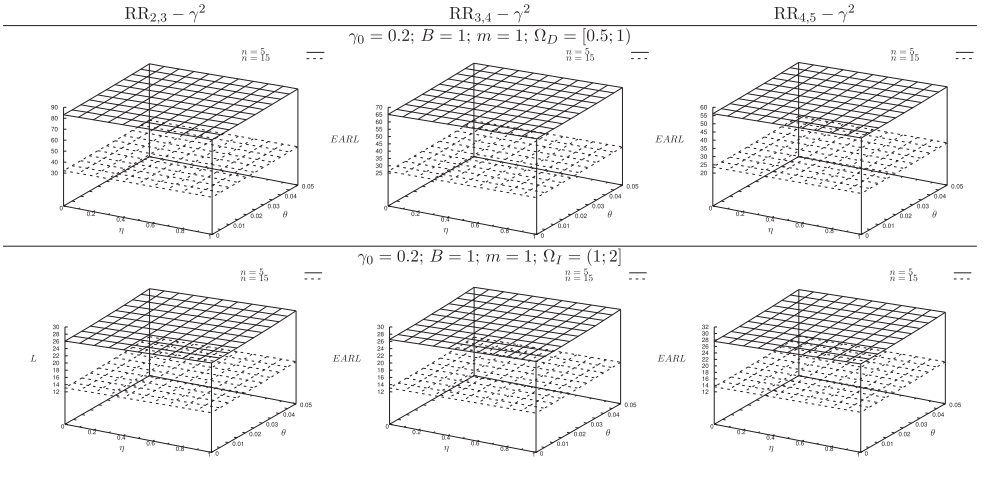

Figure 3. The effect of θ and η on the performance of the $\mathrm{RR}_{r,s} - \gamma^2$ control charts in the presence of measurement error for $\gamma_0 = 0.2$.

RR-γ^2 control charts when η varies in $[0, 1]$ and θ varies in $[0, 0.05]$ for $\gamma_0 = 0.05$ and $\gamma_0 = 0.2$, respectively. The slope of the plane which represents the *EARL* values from right to left and from outside to inside shows that the larger the values of η and θ, the larger the value of *EARL*. That is to say, these errors have negative effects on the performance

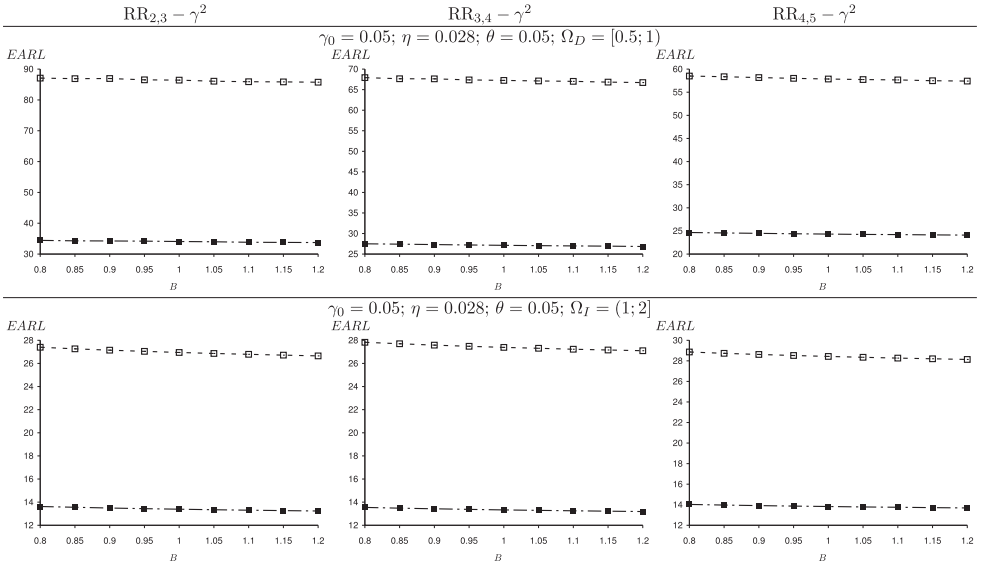

Figure 4. The effect of B on the performance of the $\text{RR}_{r,s} - \gamma^2$ control charts in the presence of measurement errors for $\gamma_0 = 0.05$; $n = 5$ (-□-) and $n = 15$ (—■—).

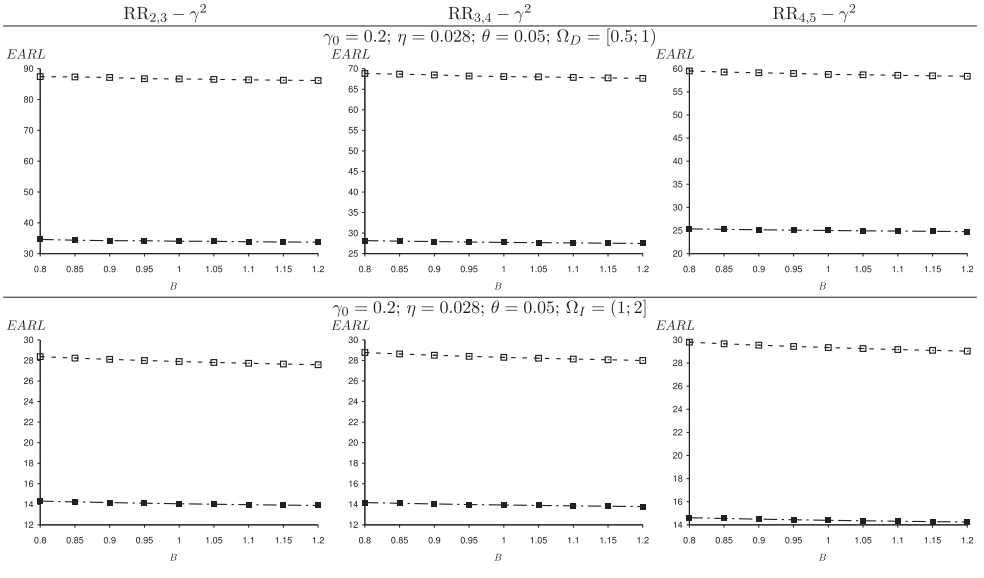

Figure 5. The effect of B on the performance of the $\text{RR}_{r,s} - \gamma^2$ control charts in the presence of measurement error for $\gamma_0 = 0.2$; $n = 5$ (-□-) and $n = 15$ (—■—).

of the RR-γ^2 charts. For example, in Figure 2 when $n = 5$, $B = m = 1$, and $\gamma = 0.05$, we have $EARL = 82.27$ for $\theta = \eta = 0$ (corresponding to no measurement errors), but $EARL = 82.81$ for $\eta = 0, \theta = 0.05$ (corresponding to the negative effect of accuracy error), $EARL = 83.42$ for $\theta = 0, \eta = 0.3$ (corresponding to the negative effect of precision error),

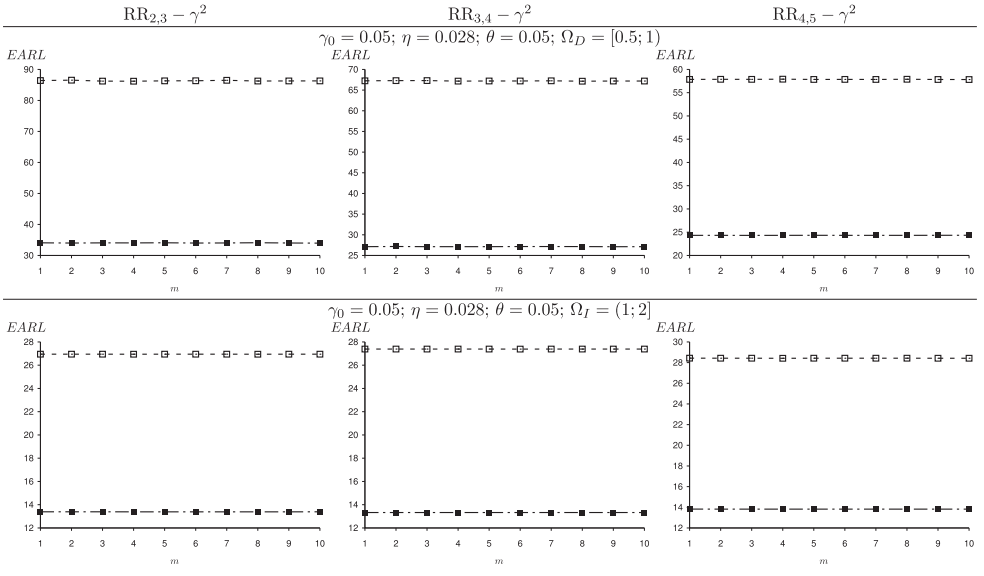

Figure 6. The effect of m on the performance of the $\mathrm{RR}_{r,s} - \gamma^2$ control charts in the presence of measurement errors for $\gamma_0 = 0.05$; $n = 5$ (-□-) and $n = 15$ (—■—).

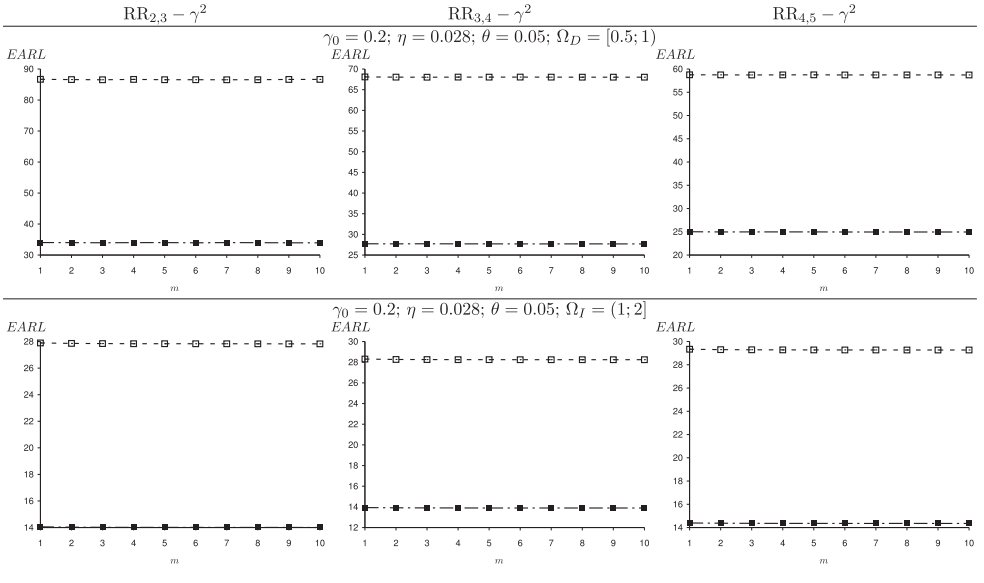

Figure 7. The effect of m on the performance of the $\mathrm{RR}_{r,s} - \gamma^2$ control charts in the presence of measurement error for $\gamma_0 = 0.2$; $n = 5$ (-□-) and $n = 15$ (—■—).

and $EARL = 84.49$ for $\theta = 0.05, \eta = 0.5$ (corresponding to the negative effect of both precision and accuracy error). The effect of B and m on the $EARL$ is displayed in Figures 4–7 for both $\gamma_0 = 0.05$ and $\gamma_0 = 0.2$. We obtain a similar trend as the case of the specific shift size: When B increases, the $EARL$ decreases and the $EARL$ does not change significantly when m increases. The almost constant $EARL$ line shows that the effect of m on these chart performance is insignificant. That is to say, increasing the value of m does not reduce the negative effect of measurement errors on the charts. In contrast, the plot of the $EARL$ corresponding to $n = 15$ is always below the plot of the $EARL$ corresponding to $n = 5$. That means, the sample size has a great impact on the $\mathrm{RR}_{r,s} - \gamma^2$ charts' performance regardless of the measurement error.

7. Illustrative example

In this section, we present an illustrative example of the implementation of the $\mathrm{RR}_{r,s} - \gamma^2$ control charts in the presence of the measurement error. The real industrial data from a sintering process in an Italian company that manufactures sintered mechanical parts, which were introduced in [5], are considered.

The process manufactures parts guarantee a pressure test by dropping time T_{pd} from 2 bar to 1.5 bar larger than 30 s as a quality characteristic related to the pore shrinkage. Since the presence of a constant proportionality $\sigma_{pd} = \gamma_{pd} \times \mu_{pd}$ between the standard deviation of the pressure drop time and its mean had been demonstrated by the preliminary regression study relating T_{pd} to the quantity Q_C of molten copper, the quality practitioners decide to monitor the CV $\gamma_{pd} = \sigma_{pd}/\mu_{pd}$ to detect changes in the process variability. According to the description in [5], an estimate $\hat{\gamma}_0 = 0.417$ is calculated from a Phase I dataset based on a root mean square computation. Phase II data are reproduced in Table 8.

Table 8. Illustrative example of Phase II dataset.

i	$\overline{X}_i^*$	S_i^*	$\hat{\gamma}$	$\hat{\gamma}^{*2}$
1	906.4	476.0	0.525	0.27563
2	805.1	493.9	0.614	0.37700
3	1187.2	1105.9	0.932	0.86862
4	663.4	304.8	0.459	0.21068
5	1012.1	367.4	0.363	0.13177
6	863.2	350.4	0.406	0.16484
7	1561.0	1562.2	1.058	1.11936
8	697.1	253.2	0.363	0.13177
9	1024.6	120.9	0.118	0.01392
10	355.3	235.2	0.662	0.43824
11	485.6	106.5	0.219	0.04796
12	1224.3	915.4	0.748	0.55950
13	1365.0	1051.6	0.770	0.59290
14	704.0	449.7	0.639	0.40832
15	1584.7	1050.8	0.663	0.43957
16	1130.0	680.6	0.602	0.36240
17	824.7	393.5	0.477	0.22753
18	921.2	391.6	0.425	0.18062
19	870.3	730.0	0.839	0.70392
20	1068.3	150.8	0.141	0.01988

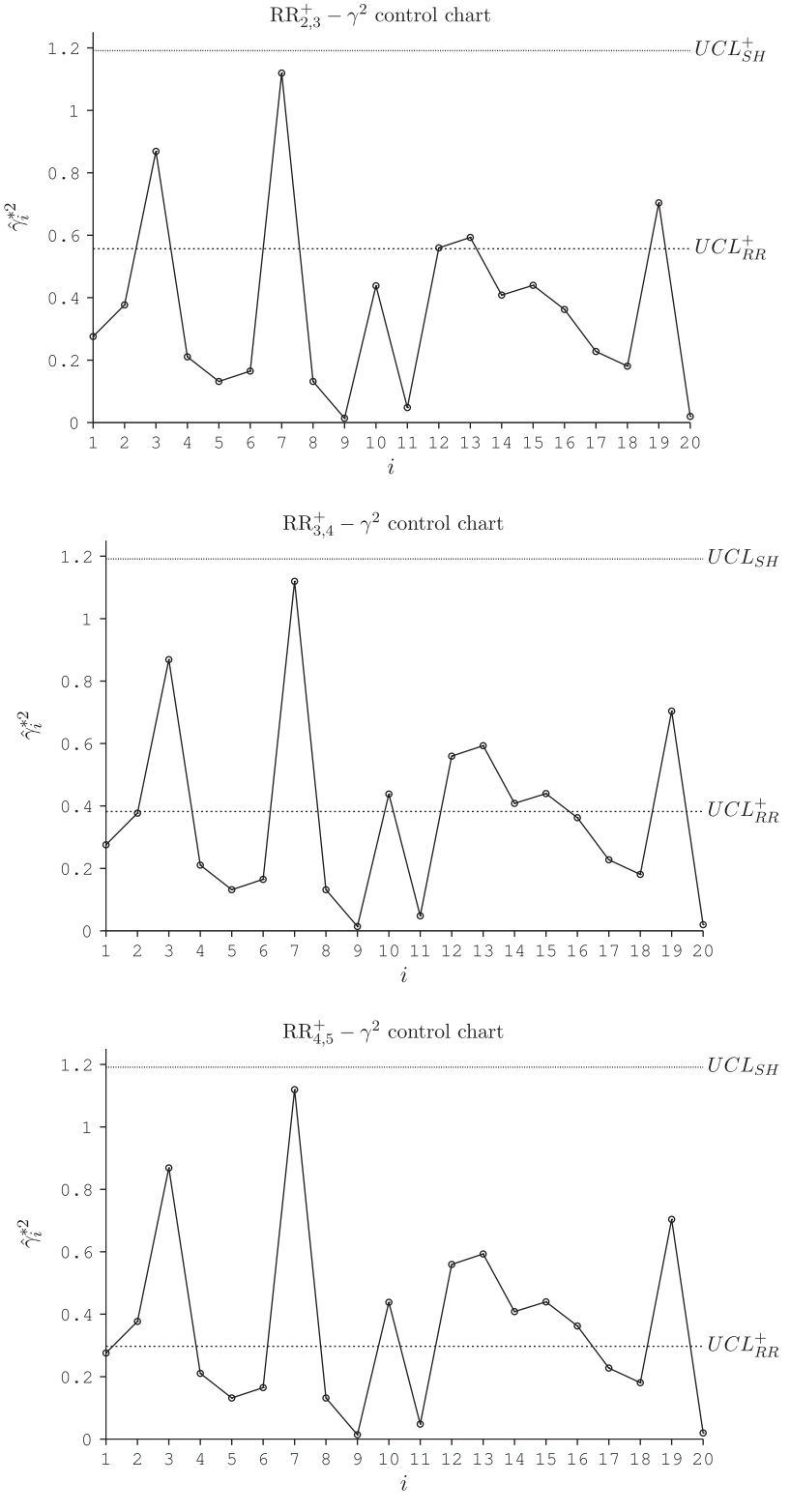

Figure 8. The upward CUSUM-γ^2 control chart in the presence of the measurement error corresponding to the Phase II data in Table 8.

According to [19] under the presence of the measurement error, we suppose that the parameters of the linear covariate error model are $\eta = 0.28$, $\theta = 0.05$, $B = 1$, and $m = 1$. Based on the process engineer's experience, a specific shift size $\tau = 1.25$ was expected to detect from the process. Therefore, we apply the upper-sided $\mathrm{RR}_{r,s-\gamma^2}$ control chart to monitor the CV squared. The control limits of the $\mathrm{RR}^{+}_{2,3} - \gamma^2$, $\mathrm{RR}^{+}_{3,4} - \gamma^2$ and $\mathrm{RR}_{4,5} - \gamma^2$ chart are found to be $UCL^{+} = 0.5567$, $UCL^{+} = 0.3821$ and $UCL^{+} = 0.2972$, respectively. The values of γ_i^{*2} are then plotted in these charts (Figure 8) long with the control limit UCL^{+}. For the purpose of comparison, we also draw the control limit ($UCL^{+} = 1.1913$) of the original Shewhart control chart with the same parameters.

As can be seen from the Figure 8, the $\mathrm{RR}^{+}_{2,3} - \gamma^2$, $\mathrm{RR}^{+}_{3,4} - \gamma^2$ and $\mathrm{RR}_{4,5} - \gamma^2$ chart signal the occurrence of the out-of-control condition by two-out-of-three, three-out-of-four, and four-out-of-five (respectively) successive plotting points above the corresponding control limits from the sample #12. Meanwhile, the Shewhart chart fails to detect this out-of-control condition.

8. Concluding remarks

In this paper, the performance of Run Rules control charts is improved slightly by monitoring the CV squared with the two one-sided charts rather than monitoring directly the CV with a two-sided chart as in a previous study in the literature. The effect of measurement errors on the performance of the $\mathrm{RR}_{r,s} - \gamma^2$ control charts using a linear covariate error model is also investigated. We have pointed out the negative effect of measurement errors on the proposed charts: the increase of η and θ leads to an increase of *EARL*. Moreover, the obtained results show that measuring repeatedly is not an efficient method for limiting these unexpected effects. Extension to Run Rules EWMA and Run Rules CUSUM γ^2 type charts and the effect of the parameters estimation on their statistical properties are suggested as further important topics of research.

Acknowledgments

The authors would like to thank the anonymous referees for their valuable suggestions that helped to improve the quality of the final manuscript. Research activities of Phuong Hanh Tran have been funded by Vietnam International Education Development – Project 911.

Disclosure statement

No potential conflict of interest was reported by the author(s).

Funding

Research activities of Phuong Hanh Tran have been funded by Vietnam International Education Development [Project 911].

ORCID

Phuong Hanh Tran http://orcid.org/0000-0002-0237-9806

References

[1] R. Breunig, *An almost unbiased estimator of the coefficient of variation*, Econ. Lett. 70 (2001), pp. 15–19.

[2] P. Castagliola, A. Achoure, H. Taleb, G. Celano, and S. Psarakis, *Monitoring the coefficient of variation using control charts with run rules*, Qual. Technol. Quant. Manag. 10 (2013), pp. 75–94.

[3] P. Castagliola, A. Achouri, H. Taleb, G. Celano, and S. Psarakis, *Monitoring the coefficient of variation using a variable sampling interval control chart*, Qual. Reliab. Eng. Int. 29 (2013), pp. 1135–1149.

[4] P. Castagliola, A. Achouri, H. Taleb, G. Celano, and S. Psarakis, *Monitoring the coefficient of variation using a variable sample size control chart*, Int. J. Adv. Manuf. Technol. 80 (2015), pp. 1561–1576.

[5] P. Castagliola, G. Celano, and S. Psarakis, *Monitoring the coefficient of variation using EWMA charts*, J. Qual. Technol. 43 (2011), pp. 249–265.

[6] Manual, *Measurement System Analysis*, 4th ed., Automotive Industry Action Group, Southfield, 2010.

[7] F. Kadri, F. Harrou, S. Chaabane, Y. Sun, and C. Tahon, *Seasonal ARMA-based SPC charts for anomaly detection: application to emergency department systems*, Neurocomputing 173 (2016), pp. 2102–2114.

[8] K.W. Khaw, M.B.C. Khoo, W.C. Yeong, and Z. Wu, *Monitoring the coefficient of variation using a variable sample size and sampling interval control chart*, Comm. Statist. Simulation Comput. 46 (2017), pp. 5722–5794.

[9] K.W. Linna and W.H. Woodall, *Effect of measurement error on Shewhart control charts*, J. Qual. Technol. 33 (2001), pp. 213–222.

[10] A.N.B. Muhammada, W. Yeong, Z. Chonga, S. Limc, and M.B.C. Khood, *Monitoring the coefficient of variation using a variable sample size EWMA chart*, Comput. Ind. Eng. 126 (2018), pp. 378–398.

[11] H.D. Nguyen, Q.T. Nguyen, K.P. Tran, and D.P. Ho, *On the performance of VSI shewhart control chart for monitoring the coefficient of variation in the presence of measurement errors*, Int. J. Adv. Manuf. Technol. 104 (2019), pp. 211–243.

[12] M. Noor-ul Amin and A. Riaz, *EWMA control chart for coefficient of variation using log-normal transformation under ranked set sampling*, Iranian J. Sci. Technol, Trans. A: Sci. 44 (2020), pp. 155–165.

[13] M. Noor-ul Amin, S. Tariq, and M. Hanif, *Control charts for simultaneously monitoring of process mean and coefficient of variation with and without auxiliary information*, Qual. Reliab. Eng. Int. 35 (2019), pp. 2639–2656.

[14] S.C. Shongwe, J. Malela-Majika, and P. Castagliola, *A combined mixed-s-skip sampling strategy to reduce the effect of autocorrelation on the X-bar scheme with and without measurement errors*, J. Appl. Stat. 5 (2020) pp. 1–25.

[15] K.P. Tran, *Run rules median control charts for monitoring process mean in manufacturing*, Qual. Reliab. Eng. Int. 33 (2017), pp. 2437–2450.

[16] K.P. Tran, *Designing of run rules t control charts for monitoring changes in the process mean*, Chemom. Intell. Lab. Syst. 174 (2018), pp. 85–93..

[17] K.P. Tran, P. Castagliola, and G. Celano, *Monitoring the ratio of two normal variables using run rules type control charts*, Int. J. Prod. Res. 54 (2016), pp. 1670–1688.

[18] K.P. Tran, H. Du Nguyen, H. Tran, and C. Heuchenne, *On the performance of CUSUM control charts for monitoring the coefficient of variation with measurement errors*, Int. J. Adv. Manuf. Technol. 104 (2019), pp. 1903–1917.

[19] K.P. Tran, C. Heuchenne, N. Balakrishnan, and M.B.C. Khoo, *On the performance of coefficient of variation charts in the presence of measurement errors*, Qual. Reliab. Eng. Int. (2018).

[20] P.H. Tran and K.P. Tran, *The efficiency of CUSUM schemes for monitoring the coefficient of variation*, Appl. Stoch. Models. Bus. Ind. 32 (2016), pp. 870–881.

[21] P.H. Tran, K.P. Tran, T.H. Truong, C. Heuchenne, P.H. Tran, and T.M.H. Le, *Real Time Data-Driven Approaches for Credit Card Fraud Detection*, Proceedings of the 2018 International Conference on E-Business and Applications, 2018, pp. 6–9.
[22] J. Ye, P. Feng, C. Xu, Y. Ma, and S. Huang, *A novel approach for chatter online monitoring using coefficient of variation in machining process*, Int. J. Adv. Manuf. Technol. 96 (2018), pp. 287–297.
[23] W.C. Yeong, M.B.C. Khoo, S.L. Lim, and M.H. Lee, *A direct procedure for monitoring the coefficient of variation using a variable sample size scheme*, Comm. Statist. Simulation Comput. 46 (2017), pp. 4210–4225.
[24] W.C. Yeong, M.B.C. Khoo, S.L. Lim, and W.L. Teoh, *The coefficient of variation chart with measurement error*, Qual. Technol. Quant. Manag. 14 (2017), pp. 353–377.
[25] F.S. Zaidi, P. Castagliola, K.P. Tran, and M.B.C. Khoo, *Performance of the hotelling T2 control chart for compositional data in the presence of measurement errors*, J. Appl. Stat. 46 (2019), pp. 2583–2602.
[26] J. Zhang, Z. Li, B. Chen, and Z. Wang, *A new exponentially weighted moving average control chart for monitoring the coefficient of variation*, Comput. Ind. Eng. 78 (2014), pp. 205–212.
[27] D. Zheng, F. Li, and T. Zhao, *Self-adaptive statistical process control for anomaly detection in time series*, Expert. Syst. Appl. 57 (2016), pp. 324–336.